

A.M.E.R.I.C.A.

Advanced Methane Emission and Regolith In-Situ Composition Analysis

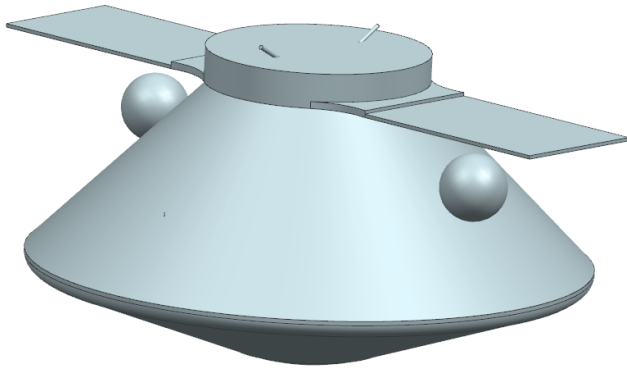
Mission Proposal



Steven Beninati, Aidan Clements, Johnathan Corbin, Matthew Dromgoole, Vish Gopalakrishnan, Kevin Iott, Sierra Koch, Jasmina Muftic, Will Parker, Vincent Putrino, Daria Stifel

MANE-4850 — Space Vehicle Design
Department of Mechanical, Aerospace, and Nuclear Engineering
Rensselaer Polytechnic Institute
December 9, 2019

I. FACT SHEET



AMERICA Cruise Stage

Destination: Medusae Fossae Formation

Vehicle Type: Lander

Cruise Stage Mass: 700 kg

Lander Mass: 396 kg

Science Mission:

AMERICA will support NASA's Mars exploration program by investigating two of NASA's science goals:

- 1) Investigate the biotic or abiotic nature of the processes that govern methane variations in the lower Martian atmosphere.
- 2) Discover the properties of martian dust and how it relates to geological formations and climate.

In support of the science mission AMERICA will carry a 60 kg suite of eight scientific instruments on board to better examine the environment, including:

- 1) The Sample Analysis at Mars to measure surface and subsurface methane.
- 2) A Robotic Arm to carry the Thermal and Electrical Conductivity Probe and the Microscopic Imager.
- 3) The Thermal and Electrical Conductivity Probe to measure the thermal and electrical properties of the martian soil.
- 4) The Microscopic Imager to determine dust grain size and type.
- 5) The Mast Camera Z to allow for visual observation of the surrounding geological formations.
- 6) The Environmental Monitoring Station to measure the ambient martian temperature and pressure.
- 7) The Modified Lunar Dust Experiment to determine the charge of martian dust particles.
- 8) The Chemistry Camera and Remote Micro-Imager will work together to determine the chemical composition of the martian regolith.

Cost:

Base: \$ 468 Million

Threshold: \$ 515.0 Million

Margin: \$ 47.0 Million

Propulsion:

Transfer: Type 1

C3: $20.5 \frac{\text{km}^2}{\text{s}^2}$

Propellant types: Nitrogen Cold Gas, Hydrazine
Engines:

- Eight Moog 058-118 Cold Gas
- Eight Aerojet Rocketdyne MR-104H

Power:

Battery Capacity: 30 Ah

Specific Energy: $141 \frac{\text{Wh}}{\text{kg}}$

Cruise Solar Panel Mass/Area: $7.32 \frac{\text{kg}}{\text{m}^2}$

Lander Solar Panel Mass/Area: $2.51 \frac{\text{kg}}{\text{m}^2}$

Schedule:

Launch Date: October 25, 2024

Landing Date: June 11, 2025

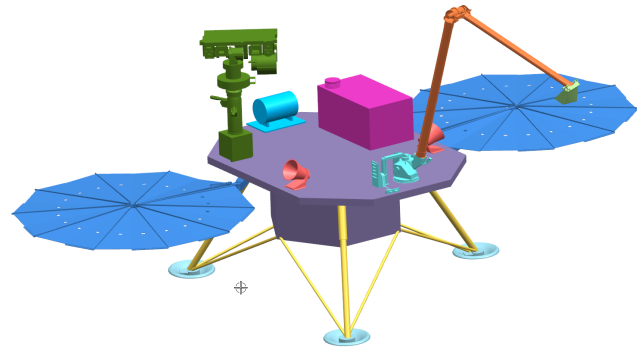
Days Active: 916

First Solar Conjunction: January 2, 2026

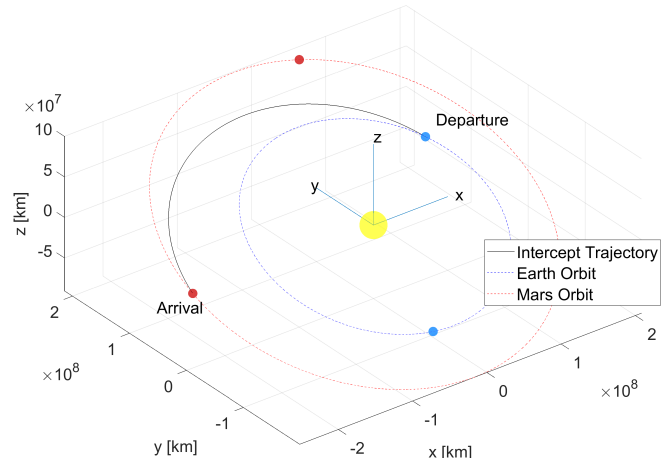
Communications:

Weekly science data generated: 240 MB

Maximum downlink rate: 512 kbps



AMERICA Lander



Planned Transfer Trajectory to Mars

Martian weather and atmospheric patterns on the global scale are not well understood. Understanding these atmospheric phenomena and variations is important to support current and future Mars exploration. The 2018 Mars Exploration Program Analysis Group (MEPAG) Science Goal II, Objective A states the need to “Characterize the fluxes and sources of dust and volatiles between surface and atmospheric reservoirs” in order to understand the present climate of Mars [16]. To work towards this goal, the Advanced Methane Emission and Regolith In-situ Composition Analysis (AMERICA) mission team has developed a mission concept that will focus on the movements of methane (CH_4) and atmospheric dust between the Martian surface and the atmosphere.

While operating in Gale crater, the Mars Science Laboratory (MSL) rover observed seasonal variations in methane levels over the course of three years [6], as well as shorter duration spikes in methane concentration [3]. Similar levels of methane have been confirmed by orbiter missions [3]. These methane variations are of particular interest because they indicate the presence of unknown processes in the Martian surface or subsurface, some of which may have a biotic origin [4].

Martian dust storms are another important component of the present Martian climate, and are still not very well understood [16]. The MEPAG 2018 Goals stress the importance of gaining a better understanding of dust behavior in the lower atmosphere for both climatology and future exploration [16].

Subsequent investigations have determined that the Medusae Fossae Formation (MFF) is potentially a large source of both methane [3] and dust [18] in the Martian atmosphere. In accordance with these findings, the AMERICA team has chosen the MFF as the landing site for a lander mission to investigate the variations of atmospheric methane and Martian dust storms.

The AMERICA mission consists of a stationary lander at the MFF which will monitor surface and near surface conditions over the course of two Martian years. The mission has two primary science goals that align with the MEPAG objectives:

- 1) Investigate the biotic or abiotic nature of the processes that govern methane variations in the lower Martian atmosphere.
- 2) Discover the properties of martian dust and how it relates to geological formations and climate.

In order to achieve Goal 1, the AMERICA lander will take regular measurements of temperature, humidity, wind speed, methane concentration, and pressure at the surface. To support these measurements, the lander will also measure subsurface methane content, water content, and temperature, using a robotic arm and scoop. The lander will also take pictures of the local geology. This will provide insight into the relationship between geological and meteorological processes and the Martian methane cycle, providing data for future missions and refinement of theories about methane processes on Mars.

In support of Goal 2, the AMERICA mission will further analyze the chemical composition of the surface regolith, and measure the thermal and electrical properties of the dust in the MFF. Images of the surrounding terrain will also be collected in order to understand the geological history of the

region and its relationship to the processes that give rise to dust storms. The science generated by the AMERICA lander will be relayed back to Earth using the Mars Reconnaissance Orbiter (MRO) and ExoMars Trace Gas Orbiter (TGO).

The AMERICA mission will provide a unique opportunity to investigate some of the least understood and most important processes on Mars. The mission profile designed by the AMERICA team will allow the monitoring of dust, methane, and atmospheric conditions on the MFF over the course of multiple seasons using reliable, flight proven hardware and instrumentation. These factors combine to create a high chance of successfully providing high value science data about the Martian climate for current and future exploration.

LIST OF FIGURES

1	Seasonal martian methane variation recorded over three years indicates a regular cyclical process	6
2	Calcium perchlorate phase change and methane release from regolith	7
3	The transfer, landing, and communication infrastructure to relay new discoveries back to Earth	10
4	AMERICA's suite of instruments will increase our understanding of Martian geologic and atmospheric processes	10
5	Science Tracibility Matrix	11
6	Contours of departure C3 for the 2024 Mars launch window	12
7	Contours of arrival V_∞ for the 2024 Mars launch window	12
8	Planned Mars transfer orbit viewed from a J2000 Sun-centered reference frame	12
9	AMERICA's approach trajectory to Mars with location of atmospheric intersection	13
10	Descent profile of entry vehicle, with parachute deployment occurring at approximately Mach 1.7 and reaching a terminal velocity of $63.5 \frac{m}{s}$	13
11	Propulsion schematic for cruise stage using N_2 and having $30 \frac{m}{s}$ for trajectory changes	14
12	Propulsion schematic for landing stage using hydrazine as a propellant and helium as a pressurant for the skycrane and powered decent procedure and executing ΔV_s of $199.59 \frac{m}{s}$ and $403.31 \frac{m}{s}$ respectively	14
13	Cruise stage	16
14	Sky Crane isometric and bottom views	17
15	AMERICA skycrane concept of operations	18
16	Lander in deployed configuration [70] [71] [72]	18
17	Lander in stowed configuration	18
18	Schematic of the robotic arm from a side view. White cylinders represent joints and black rectangles are lengths of the arm	18
19	Sampling area of robotic arm	18
20	Orbits of the satellites used as communication relays	20
21	Data downlink per orbiter over one sol	21
22	Data downlink transfer volume per sol over a typical martian year	22
23	System interconnect diagram	24
24	Deployable Flexible Solar Array sequence that will be used to open solar panels to proper position [41]	24
25	Power profile of surface operations during cycle of 7 sols	24
26	Power Breakdown	25
27	AMERICA lander risk matrix outlining the priority of the risks based on the severity of consequence and the probability of occurrence	26
28	AMERICA's functional organizational structure promotes communication and teamwork between similar subsystems. To overcome communication barriers between subsystems whole team meetings occurred four times a week.	27
29	Gantt chart for full mission schedule of AMERICA	29

LIST OF TABLES

I	Mission priority for measurements that can be descoped	8
II	Measurement intervals for baseline and threshold missions	8
III	SAM Specifications [21]	8
IV	TECP Specifications	8
V	Microscopic Imager Specifications [28]	9
VI	Mast Camera Z Specifications [29]	9
VII	EMS Specifications [30]	9
VIII	MLDEX Specifications [31]	9
IX	ChemCam & RMI Specifications [32]	10
X	Cruise Stage Overview	14
XI	Landing Stage Overview	15
XII	Honeywell MIMS IMU [38]	15
XIII	Ball CT2020 [68]	15
XIV	Bradford Coarse Sun Sensor [67]	15
XV	LWRHU Specifications [44]	15
XVI	WEB Components [44]	16
XVII	Lander Mass Distribution	17
XVIII	Uplink and downlink frequency bands for the UHF and X band communication systems	19
XIX	Coherent doppler data tracking service schedule	20

XX	Delta-DOR tracking services schedule	20
XXI	Example link budgets for communication links with each AMERICA antenna ¹	21
XXII	Data rates and Eb/N0 for links not shown in table XXI	21
XXIII	Solar Array Attributes [40]	23
XXIV	Battery Cell Attributes [42]	23
XXV	AMERICA Cost Model	29
XXVI	Individual Member Contributions	33

CONTENTS		
I	Fact Sheet	1
II	Science Investigation	6
II-A	Overview	6
II-A1	Introduction	6
II-A2	Fundamental Questions . . .	6
II-A3	Landing Site Selection . . .	7
II-B	Needs, Goals, and Objectives	7
II-C	Science Tracibility Matrix	7
II-D	Baseline and Threshold Science Mission	7
II-E	Proposed Instrumentation	8
II-E1	Sample Analysis at Mars (SAM)	8
II-E2	Robotic Arm (RA)	8
II-E3	Thermal and Electrical Conductivity Probe (TECP)	8
II-E4	Microscopic Imager (MI)	9
II-E5	Mast Camera Z	9
II-E6	Environmental Monitoring Station (EMS)	9
II-E7	Modified Lunar Dust Experiment (MLDEX)	9
II-E8	Chemistry Camera (Chem-Cam) and Remote Micro-Imager (RMI)	9
II-F	Concept of Operations	10
III	Mission Implementation	12
III-A	Navigation and Landing	12
III-A1	Astrodynamic	12
III-A2	Entry, Descent, and Landing (EDL)	13
III-A3	Thermal Protection System (TPS)	14
III-A4	Propulsion	14
III-A5	Attitude Determination and Control System (ADCS) . .	15
III-B	Thermal Control System	15
III-C	Mechanical Design	16
III-C1	Cruise Stage and Entry Vehicle	16
III-C2	Sky Crane	16
III-C3	Lander	16
III-C4	Robotic Arm	17
III-D	Communications	17
III-D1	Overview	17
III-D2	Hardware	17
III-D3	Critical Event Telemetry and Solar Conjunction	19
III-D4	Link Budgets	19
III-D5	Tracking Telemetry	20
III-E	Command and Data Handling (C&DH)	20
III-E1	Data Collection & Uplink Schedule	20
III-E2	Data Collection Modes	22
III-E3	Hardware	22
III-F	Power	23
IV	Management	26
IV-A	Risk Classification	26
IV-B	Risk Mitigation	26
IV-C	Technical Risk Analysis	26
IV-D	Organizational Chart	26
IV-E	Safety and Quality Assurance	27
IV-E1	Contamination Control	27
V	Cost and Schedule	28
V-A	Cost Estimate	28
V-A1	Proposed Mission Cost	28
V-B	Gantt Chart (Full Mission Lifecycle)	28
VI	References	30
VII	Appendix	33

II. SCIENCE INVESTIGATION

A. Overview

1) *Introduction:* Methane (CH_4) is an organic compound common in Earth's atmosphere. A majority of the terrestrial sources of methane are produced by living organisms, while the rest are attributed to a variety of Earth's geological processes [1]. Special scientific interest, therefore, has been devoted to exploring the existence of methane on the surface and in the lower atmosphere of Mars. Measurements from earth-based telescopes, as well as in-situ orbiters and landers have consistently verified the existence of methane on Mars, but vast temporal inconsistency in its atmospheric concentration remains largely unexplained. Methane only has a lifetime of approximately 300 years in the oxidizing atmosphere of Mars, which means that today's methane must have been either recently produced or continuously replenished [2]. Figure 1 shows a consistent variation in atmospheric methane concentration recorded over three years [6].

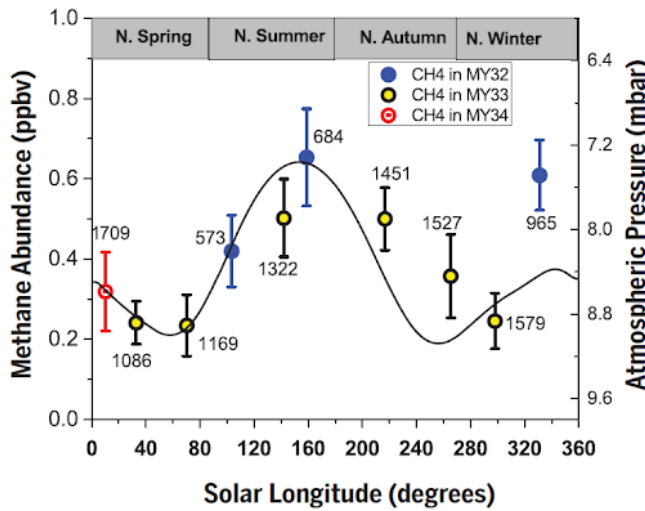


Fig. 1. Seasonal martian methane variation recorded over three years indicates a regular cyclical process

Sporadic spikes in methane concentration from a baseline of ≈ 0.7 parts per billion by volume (ppbv) to nearly 21 ppbv have been measured locally by landers and orbiters since arrival [3]. Additionally, a more modest but consistent seasonal variation in atmospheric methane concentration has been observed. The processes which govern these sporadic and seasonal releases are believed to be largely independent, but neither is well understood. There is a pressing push in the scientific community to collect more atmospheric data from the surface of Mars to address these pressing questions. This data will play a crucial role in helping to understand the context in which martian methane exists, and the mechanism by which it is exposed to the atmosphere.

If it is determined that martian methane is biotic in origin, our fundamental understanding of life in the universe and the conditions that support it will change. If evidence supports geological origins, a significant improvement in awareness of the subterranean processes of the planet will result.

The process by which dust is transferred into the martian atmosphere is as poorly understood as the atmospheric transfer process for methane. Martian dust storms have been known to propagate quickly and even occasionally envelop the planet. In June of 2018, contact with the Opportunity rover was lost after a dust storm occluded the sun and prevented the vehicle from charging its batteries [15]. The loss of Opportunity provides an example of the danger these storms pose. A better understanding of the processes which govern martian dust storms is necessary to better predict their behavior and protect our high value (both scientifically and monetarily) resources on Mars' surface.

Currently, martian weather models are insufficient for accurately predicting atmospheric trends affecting dust storm propagation [16]. More weather stations are necessary in order to close this gap in capability. Additionally, an improved understanding of dust properties is necessary to predict the impact dust storms will have on the complex mechanical and electrical systems operating on Mars.

2) *Fundamental Questions:* The Advanced Methane Emission and Regolith In-situ Composition Analysis (AMERICA) Mars lander mission will help to answer several of the scientific community's fundamental questions relating to the martian atmosphere and geology.

a) *Is the source of martian methane biotic or abiotic?:* This topic has recently received significant media attention, and sparked new national interest in the planetary science being done on Mars. Experiments on Earth have shown that by measuring the relative abundance of CH_4 and H_2 in subsurface serpentinization processes, it is possible to determine whether the methane source is likely biotic or abiotic [17]. Analysis of this type can be of use in answering the question of the methane's origin on Mars. The AMERICA lander will provide scientists with the data necessary to support reasonable conclusions.

b) *How do we explain both seasonal and sporadic methane releases?:* Seasonal atmospheric methane variation has consistently been observed, and one theory explaining this variation points to the deliquescence of perchlorate salts in the shallow subsurface of martian regolith [18]. Corresponding with temperature and humidity increases at the surface, the deliquescence of these perchlorates is predicted to release methane, while the dry perchlorates adsorb atmospheric methane during other times of year, shown graphically in figure 2 [18]. By collecting information about the temperature and humidity of the surface, as well as perchlorate concentration and state within the regolith, it will be possible to ascertain whether this theory has merit.

One theory explaining the sporadic release of methane in Mars' atmosphere contends that subsurface permafrost holds methane, which is episodically released along fault lines during periods of high geological activity [3]. This theory is supported by measurements taken from the Curiosity rover and Mars Express Orbiter during methane spikes. Deep subsurface aquifers and even microorganisms (extinct or extant) are among possible sources for the methane released by the permafrost in this scenario. However, more in-situ data

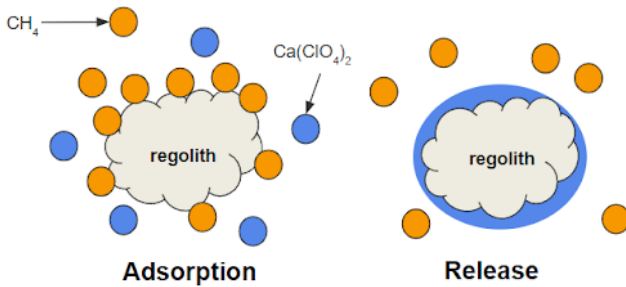


Fig. 2. Calcium perchlorate phase change and methane release from regolith

collection from predicted source locations is necessary to fully test the validity of these theories [18].

c) **How do martian dust storms propagate?**: During dust storms, individual grains of dust and sand are charged by collisions. The resulting electrical fields and induced currents on these grains are predicted to perhaps play a role in lifting stationary dust and contributing to the propagation of massive dust storms [16]. Understanding these electrical properties of Martian dust is necessary to increase our capability to model and predict these dangerous storms.

3) **Landing Site Selection**: A landing site within the Medusae Fossae Formation (MFF, 3.2° S, 163° W) was selected since it was found to be the location with the highest potential to answer the fundamental questions the AMERICA lander seeks to answer. First, the MFF is a geologically active region with a layer of shallow ice below the surface [3]. Prevailing theories about sporadic methane release predict that those conditions are ideal for observing large methane spikes. Second, the MFF exists in a region distant enough from other landers and rovers to make measurements here unique from measurements taken, perhaps in tandem, elsewhere on Mars’ surface. Third, it is believed that the MFF is the largest source of dust for Martian dust storms, which will make it easy to measure the electrical properties of the dust in the surrounding region, since dust storms are so common here [19]. Together, these three factors make the MFF an ideal landing location particularly suited well for this mission.

B. Needs, Goals, and Objectives

Based on the science questions discussed above, the AMERICA team has established several science needs, goals, and objectives that align with NASA’s Strategic Plan 2018 and the Mars Exploration Program Analysis Group (MEPAG) Mars Science Goals, Objectives, Investigations, and Priorities: 2018 that pertain to these central questions.

Need: Understand the processes and history of the climate and geology on Mars. (Strategic Plan 2018 Objective 1.1) [20]

a) **Goal I**: Investigate the biotic or abiotic nature of the processes that govern methane variations in the lower Martian atmosphere. (MEPAG Goal 1, Sub-Objective B3) [16]

Objectives:

- 1) Characterize methane prevalence and profile atmospheric conditions (humidity, wind speed, pressure, temperature) over time at the **surface**. (MEPAG Goal 2, Investigation A1.1) [16]
- 2) Measure **subsurface** methane content, water content, and temperature over time. (MEPAG Goal 1, Investigation B3.1) [16]
- 3) Visually inspect landscape for signs of processes related to methane release (MEPAG Goal 1, Investigation B3.3) [16]

b) **Goal II**: Discover the properties of martian dust and how it relates to geological formations and climate. (MEPAG Goal 2, Sub-Objective A.1) [16]

Objectives:

- 1) Measure physical and chemical composition of surface regolith at landing location. (MEPAG Goal 3, Investigation A1.6) [16]
- 2) Determine physical and electrostatic properties (charge on individual grains, electrical/thermal conductivity) of dust. (MEPAG Goal 2, Investigation A1.2) [16]
- 3) Visual inspection of geological formations and samples near landing site. (MEPAG Goal 3, Investigation A2.3) [16]

C. Science Tracibility Matrix

In order to address the Needs, Goals, and Objectives described in section II-B, the AMERICA team has identified several measurements that can be taken at the MFF. These measurements have been organized in the science traceability atrix shown on page 11. Any mission descopes are listed in the science traceability matrix. The “baseline” measurement listed is the fully scoped mission, and the “threshold” measurement corresponds to the minimum requirements for the AMERICA mission to be considered successful. The threshold science mission is further discussed in section II-D.

D. Baseline and Threshold Science Mission

In order to account for unexpected restrictions on cost, power, and mass budgets, the AMERICA mission profile contains several descopes that are designed to reduce power consumption, cost, mass, or some combination of the three. For example, the science traceability matrix provides both a “baseline” and a “threshold” value for several instruments and measurement criteria. The threshold criteria require lower resolution measurements, which allows the AMERICA mission to use cheaper, less precise instrumentation, should the need arise. The decision to switch instruments will be made very early in the design process, once a total mission cost estimate has been determined. If the cost exceeds the mission budget, the instruments will be descoped based on lowest mission priority. The priority of measurements that can be descoped is shown in table I. The lowest priority measurements will be descoped first. In table I, a lower number represents a higher priority measurement.

TABLE I
MISSION PRIORITY FOR MEASUREMENTS THAT CAN BE DESCOPED

Measurement	Priority
Methane concentration	1
Dust particle charge	2
Dust particle size	3
Geological feature images	4

Another form of mission descope for the AMERICA mission is the frequency of measurements. This decision can be made at any time during the mission, and so provides a flexible option to save power and data transmission cost. The baseline and threshold measurement intervals for descopable measurements are shown in table II.

TABLE II
MEASUREMENT INTERVALS FOR BASELINE AND THRESHOLD MISSIONS

Measurement	Baseline Interval	Threshold Interval
SAM	6 hrs each sol	24 hrs each week
Temperature & Pressure	5 min each hr	5 min every 2 hr
MastCam & MI	5 images weekly	3 images weekly
TECP	75 mins each sol	45 mins each sol

E. Proposed Instrumentation

The AMERICA lander will carry the science instrument payload described in the following sections to collect the data specified in the science traceability matrix. This instrument payload consists of instruments similar to those flown on other deep space missions. These types of instruments have already proven to be reliable, increasing the likelihood the AMERICA mission will be able to achieve its science objectives.

1) *Sample Analysis at Mars (SAM)*: The Tunable Laser Spectrometer (TLS), Quadrupole Mass Spectrometer (QMS), and a Gas Chromatograph (GC) together form the SAM instrument and are needed to measure the surface and subsurface methane present in the Martian environment. The specifications regarding SAM capabilities are defined in table III.

TABLE III
SAM SPECIFICATIONS [21]

Property	Value
Mass	40 kg
Volume	76 cm x 44 cm x 43 cm
Power	375 W (peak)
Data Volume	30 MB
Spectral Range	3721 nm - 3270 nm 3057.6 cm ⁻¹ - 3058 cm ⁻¹

To measure the atmospheric methane abundance, the SAM instrument utilizes a Chemical Separation and Processing Laboratory (CSPL) to extract an appropriate sized gas sample through a system of inlet tubes, valves, pumps, gas reservoirs, and regulators [22]. The solid samples used to measure subsurface methane are delivered to SAM through the Solid Sample Inlet System (SSIT) and are sieved into the Sample

Manipulation System (SMS) [21]. The SMS consists of 74 sample cups that hold the soil samples, which will then be baked by the GC to release the gases [21]. The gases will be identified through the surveying ability of the QMS, while the TLS will target specific gases, such as methane or hydrogen and oxygen , to determine the ratio of their isotopic species [21]. This information will contribute to the methane research as well as the search for water on Mars.

2) *Robotic Arm (RA)*: The Robotic Arm (RA) is required to carry two science payloads, the Thermal and Electrical Conductivity Probe (TECP), and the Microscopic Imager, as well as a scoop to acquire regolith/ice samples from the surface surrounding the lander. The RA will have 5 degrees of freedom and will span a total of 2.4 m.

To acquire samples of the Martian soil, the scoop will interact within the workspace area that is bounded by a maximum radius 2.4 m from the arm's base on the lander. Solid samples are collected through the front chamber of the scoop and are then transferred to the required target instruments [25]. If the scoop encounters ice, the scoop will first deploy a knurled grip to prevent motion, and then the scoop will energize a rasp cutting tool to continuously penetrate the surface and break the ice dense soil [25]. Ice samples are collected from the plume created by the rasp cutting tool through the rear chamber [25]. Additionally, the RA will position the TECP to take measurements of thermal and electrical conductivity, and wind speed, as well as position the Microscopic Imager to determine the size of individual grains of Martian dust.

3) *Thermal and Electrical Conductivity Probe (TECP)*: The Thermal and Electrical Conductivity Probe will complete measurements on the thermal and electrical properties of the Martian dust/soil, and well as the wind speed above the surface. The needles on the instrument allow for data acquisition on the temperature, thermal conductivity, electrical conductivity, and electric permittivity of the soil. The standard specifications for the TECP instrument are listed in table IV.

TABLE IV
TECP SPECIFICATIONS

Property	Value
Mass	1 kg [26]
Volume	118.76 mm x 40.64 mm x 16.64 mm [13]
Power	6.6 W (peak) [26]
Data Volume	12 bits [26]

To acquire data on the electrical and thermal properties, the TECP needles are inserted into the regolith. Accurate measurements depend on uniform and linear needle insertion [27]. Two needle pairs take electrical measurements when acting as electrodes, and thermal data is taken when the pairs act as thermometers and heating elements [27]. These measurements are taken for several minutes [26]. The needles of the TECP are held aloft above the surface to take wind speed measurements, which are monitored by heating one needle for 70 seconds and following the cooling of the needle for 90 seconds afterward [27].

4) *Microscopic Imager (MI)*: The Microscopic Imager (MI) provides a means to closely analyze the regolith to determine the grain size and type. Information on the Microscopic Imager's size, and capabilities is listed in table V.

TABLE V
MICROSCOPIC IMAGER SPECIFICATIONS [28]

Property	Value
Mass	0.29 kg
Volume	48.6 mm x 51 mm x 41 mm (MI optics) 78 mm x 75.1 mm x 34 mm (electronics box)
Power	4.3 W
Data Volume	13 Mbits

In order to record data on the grain size of Martian soil the Microscopic Imager will be mounted on the RA. This will allow the instrument to be positioned properly above a sample. The MI will gather images which it can then analyze at higher magnification, which can scale down to as small as 2 pixels ($84\mu\text{m}$) wide by $500\mu\text{m}$ long [28]. The magnification available through the MI will allow for characterization of the grain size.

5) *Mast Camera Z*: A single Mast Camera comprised of two cameras will be mounted on the lander to allow for visual observation of the geological formation present as well as the lander's surroundings at the MFF. The two cameras allow for the Mast Camera to capture depth and three dimensional images. These qualities are supportive of the geological analysis that will be conducted. Table VI reviews the Mast Camera Z specifications and capabilities.

TABLE VI
MAST CAMERA Z SPECIFICATIONS [29]

Property	Value
Mass	4.5 kg (total) 1.25 kg (each camera head)
Volume	11 cm x 12 cm x 26 cm (each camera) 22 cm x 12 cm x 5 cm (electronics)
Power	17.4 W (each)
Data Volume	11 bits/pixel
IFOV	0.5 - 0.15 mm/pixel @ 2 m 2.7 - 0.74 cm/pixel @ 100 m
Wavelength Range	400 - 1000 nm

The Mast Camera Z is a direct descendant of the Mastcam utilized on Mars Science Laboratory (MSL) with increased zoom abilities [29]. Each camera head will be capable of producing red/blue/ green (RBG), narrow-band visible/near-infrared (VNIR) color, and direct solar images within a field of view between 5° to 15° [29]. The science data collected will be in the form of full-frame images, sub-framed images, thumbnails, and videos of groups of pictures, which will be returned in the form of color JPEG images/thumbnails, losslessly-compressed images, compressed color videos, and raw 11-bit images [29].

6) *Environmental Monitoring Station (EMS)*: The Environmental Monitoring Station (EMS) on the lander consists of a Barocap® sensor head and the corresponding Thermocap®

sensor heads distributed by Vaisla [30]. The EMS will measure the ambient surface temperature and pressure by the lander. The abilities and design specifications of the EMS are listed in table VII.

TABLE VII
EMS SPECIFICATIONS [30]

Property	Value
Mass	0.04 kg
Volume	62 mm x 50 mm x 1mm
Power	15 mW
Data Volume	1 MB (per 3 hour measurement period)
Accuracy	0.1 Pa (Pressure) 1 - 4.5 K (Temperature)

The EMS determines the atmospheric pressure through a pressure sensitive membrane that bases the pressure off of the distance between two capacitor plates [30]. The distance changes due to pressure, then in turn changing the capacitance of the pressure head. The EMS is expected to take observations of the ambient conditions for a period of 5 minutes each hour, and occasional longer measurements taken over the course of 1 hour continuously [30]. The total expected time of observation allocated to the EMS in the first 100 sols is expected to be 2 - 10 hours per sol, and will vary depending on the available power and data [30].

7) *Modified Lunar Dust Experiment (MLDEX)*: The Modified Lunar Dust Experiment (MLDEX) adjusts the Lunar Dust Experiment utilized in the Lunar Atmosphere and Dust Environment Explorer (LADEE) mission. It will be introduced on the AMERICA lander in order to determine the charge of the Martian dust particles. Table VIII describes MLDEX specifications.

TABLE VIII
MLDEX SPECIFICATIONS [31]

Property	Value
Mass	3 kg
Volume	15 cm x 15 cm x 25 cm
Power	5 W
Data Volume	1 kbit/s

The MLDEX instrument is an impact ionization dust detector. When a dust particle impacts the target within the MLDEX instrument it generates a plasma cloud which will in turn create an electric field to separate the ions and electrons [31]. The electrons are then collected on the hemispherical target and measured by a charge sensitive amplifier [31]. Thus, the MLDEX instrument determines dust charge when the moving dust impacts with the 0.01 m^2 area target found in the rear of the mechanism [31].

8) *Chemistry Camera (ChemCam) and Remote Micro-Imager (RMI)*: The ChemCam and RMI will sample the surrounding soil and rock to determine the chemical composition of the regolith. Information pertaining to ChemCam is found in table IX.

The ChemCam determines the chemical structure of the Martian soil through the Laser Induced Breakdown Spec-

TABLE IX
CHEMCAM & RMI SPECIFICATIONS [32]

Property	Value
Mass	10.791 kg
Volume	384 mm x 219 mm x 166 mm (Mast Unit) 197 mm x 236 mm x 154 mm (Body Unit)
Power	64.7 W
Data Volume	12.9 kB
Spectral Range	240 - 840 nm

troscopy (LIBS) process in which brief high powered laser pulses are focused on a portion of the rock/soil [32]. The laser pulses ablate the rock and release a plasma that is collected by a telescope and transmitted to the spectrometers in the body unit through a fiber optic cable [32]. The LIBS spectrometers cover a spectrum from ultraviolet to near infrared [32]. The RMI is included to capture contextual images (350–550 μm) of the observation points that the LIBS portion of the instrument investigates [32].

F. Concept of Operations

The AMERICA mission is designed to understand the processes and history of climate on Mars by analyzing possible sources of methane and the geological composition/formation in the Medusae Fossae Formation (MFF). At the end of phase D, the launch vehicle will place the AMERICA spacecraft on an intercept trajectory to Mars. The spacecraft will take a direct entry approach into the Martian atmosphere, utilizing a thermal protection system to protect equipment from the extreme temperatures of atmospheric entry. A powered descent will position the AMERICA lander in a suitable location within the MFF, providing access to Martian soil to perform surface and subsurface data collection.

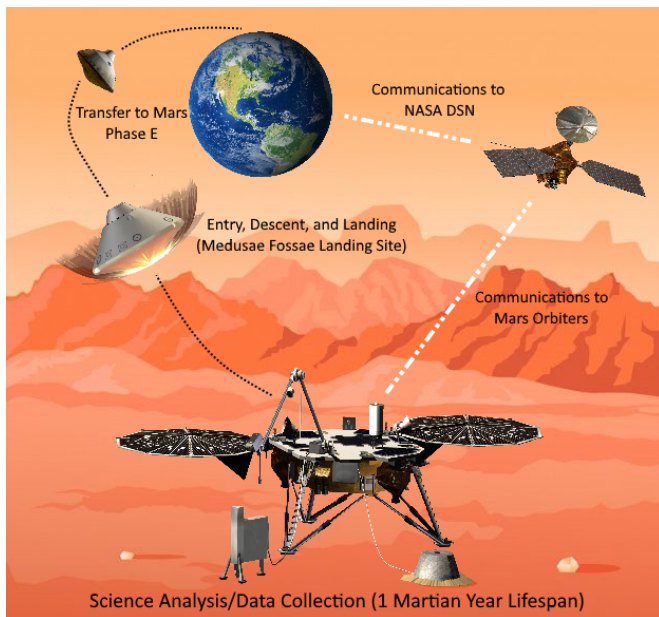


Fig. 3. The transfer, landing, and communication infrastructure to relay new discoveries back to Earth

The lander will then proceed with phase E by providing a platform to measure methane prevalence in the surface and subsurface, investigate sources of methane release, determine the electrostatic properties of dust, measure the chemical composition of the surface regolith, and visually document the surface geology. Collected data will be broadcast to Mars orbiters which will then relay science data to the NASA Deep Space Network (DSN). Data upload shall occur for at least one Martian year, the design life of the lander, and closeout, or phase F, will begin. The concept graphic figure 3 depicts the flow of travel, communication, and data handling, while figure 4 depicts various scientific data that will be collected.

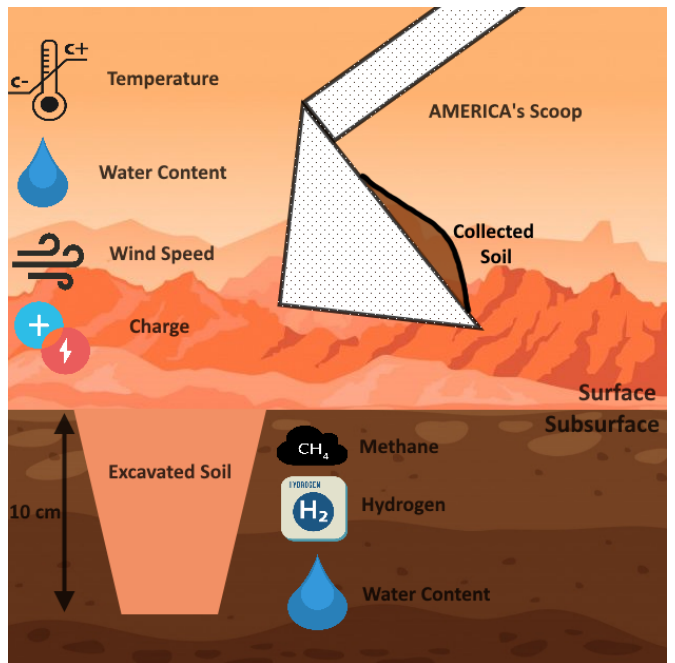


Fig. 4. AMERICA's suite of instruments will increase our understanding of Martian geologic and atmospheric processes

Science Goals	Science Objectives	Scientific Measurement Requirements		Instrument Requirements			Projected Performance	Mission Requirements (Top Level)
		Physical parameters	Observables					
GOAL 1	Objective 1	Atmospheric Methane Concentration	Spectroscopic Lines	Concentration detection	0.2 ppbv - 60 ppbv [4] (Baseline)	5 ppbv - 30 ppbv [5] (Threshold)	0.2 ppbv - 60 ppbv [4]	Successful soft landing on Medusae Fossae
				Spectral Range	3057.5 cm^-1 and 3058.0 cm^-1 [6] (Baseline)	3000 cm^-1 and 3030 cm ^-1 [5] (Threshold)	3057.5 cm^-1 and 3058.0 cm^-1 [6]	
				Spectral Resolution	0.0005 cm^-1 [6] (Baseline)	1.3 cm^-1 [5] (Threshold)	0.0005 cm^-1 [6]	
		Surface Atmospheric Conditions	Temperature	Temperature range [7]	-133.15K - 303.15 K with 4.5K accuracy at 213K and 1k at 273 K		210.15 K	
				Pressure	700 Pa - 900 Pa with .10Pa accuracy		740 Pa	
			Water Content	Concentration detection [8]	Wavelength: 240nm Resolution: 0.3nm		Wavelength: 240 nm -950 nm Resolution:.09 nm - 0.30 nm	
			Wind velocity	Wind speed [7]	0 m/s - 30 m/s with accuracy of 50% of wind speed		5 m/s	
				Wind direction [7]	20 deg of resolution from 250 degrees to 50 degrees		360 degrees	Ability to define baseline location and orientation
	Objective 2	Subsurface Methane Concentration	Spectroscopic Lines	Concentration detection	0.2 ppbv - 60 ppbv [4] (Baseline)	5 ppbv - 30 ppbv [5] (Threshold)	0.2 ppbv - 60 ppbv [4]	Capability to penetrate surface 15cm
				Spectral Range	3057.5 cm^-1 and 3058.0 cm^-1 [6] (Baseline)	3000 cm^-1 and 3030 cm ^-1 [5] (Threshold)	3057.5 cm^-1 and 3058.0 cm^-1 [6]	
				Spectral Resolution	0.0005 cm^-1 [6](Baseline)	1.3 cm^-1 [5](Threshold)	0.0005 cm^-1[6]	
		Subsurface Conditions	Water Content	Concentration detection [7]	Wavelength of Light: 240.8 nm - 905.5 nm		Between 0.09 nm and 0.30 nm	
			Temperature	Temperature range [8]	110 K - 220 K with .10 K accuracy		12 mK	
GOAL 2	Objective 3	Type of feature	Images of geologic formations	Image resolution	.074 mrad/pixel (Baseline) [9]	.25 mrad/pixel (Threshold) [10]	.074mrad/pixel [9]	Ability to view regolith samples
				Spectral range	0.4 um-1.0 um [10]		0.4 um -1.0 um [10]	
		Chemical composition of regolith	Chemical profile	Spectral range and resolution [8]	240 nm-675 nm at resolution 0.3nm		240 nm - 850 nm at resolution 0.09-0.3nm	
			Surface description	Focal length [11]	21 mm - 68 mm		68mm	
	Objective 2	Electrostatic dust properties	Grain size/type	Image size [11]	1.5 mrad/pixel [11]	focal length 21 mm [11]	1.5 mrad/pixel [11] focal length 21 mm [11]	Capability to penetrate surface up to 15 cm
				Charge	< 1μm (baseline)	< 5μm (threshold)	< 0.25μm	
				Charge range [12]	< 2.4e5 e- (baseline)	< 3e7 e- (threshold)	> 3700 e-	
			Electrical conductivity	Electrical Conductivity [13]	Range: 1 - 10e7 nS/cm		55nS/cm - 715 nS/cm	
		Thermal dust properties	Permittivity	Relative permittivity range [13]	Range: 1-20 Resolution: 0.005		Range: 1-20 Resolution: 0.005	
			Thermal conductivity	Thermal Conductivity [13]	Range: 0.03 W/(m K)- 2.5 W/(m K)	Accuracy: ±10%	2.0 ± 1.0 W/(m K)	
	Objective 3	Visual characteristics of geological formations	Images of samples from landing site	IFOV [11]	31 um/pixel		31 um/pixel	Unobstructed view of surrounding land
			Images of nearby geological formations	IFOV [14]	.074 mrad/pixel (Baseline) [9], focal length: 1km	0.24 mrad/pixel (Threshold) [14], focal length: 1km	0.24 mrad/pixel	

III. MISSION IMPLEMENTATION

A. Navigation and Landing

1) *Astrodynamic*: In order to perform the science investigation necessary for the AMERICA lander to accomplish the mission requirements, a soft landing on the Martian surface is required. From an astrodynamics perspective, a soft landing on Mars requires careful consideration to be placed on available launch windows that not only maximize the total mass placed on Mars, but also minimize the velocity of the spacecraft upon arrival at Mars for a given launch vehicle.

To assess the viability of various launch and arrival times, plots of departure C3 and arrival velocity for an Earth-Mars transfer were analyzed. With a deadline of launching by September 20, 2025, feasible launch windows were analyzed between the beginning of the year 2022 and the launch deadline. 2024 was chosen as the launch window for analysis in order to allow time for the vehicle to be fully designed and constructed. Figures 6 and 7 show contour plots of C3 and V_∞ , respectively, for the launch window within 2024.

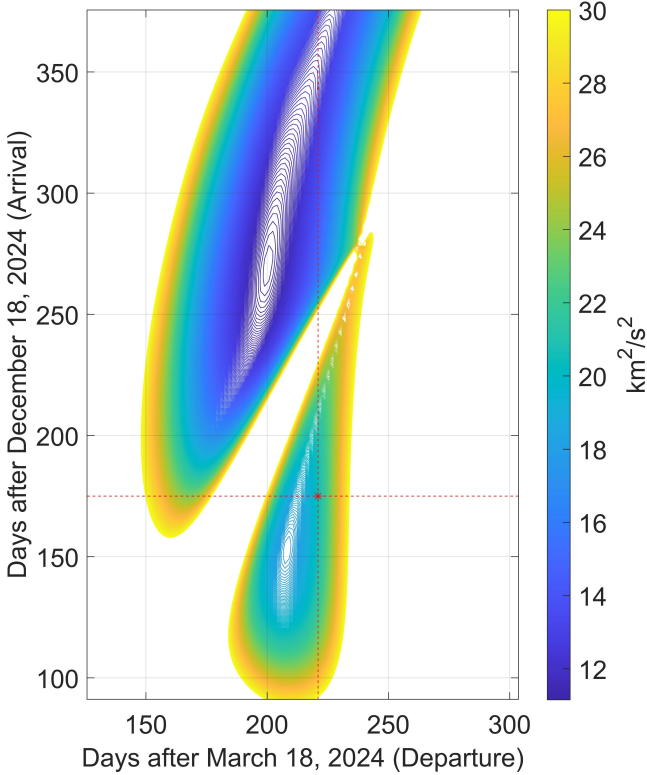


Fig. 6. Contours of departure C3 for the 2024 Mars launch window

A type 1 transfer orbit ($< 180^\circ$) was chosen to ensure consistent contact with Earth at an adequate signal-to-noise ratio. Additionally, a type 1 transfer reduces the time of flight for the cruise stage, which will decrease the chances of failure occurring while the spacecraft is exposed to the environment of space. The proposed launch date and arrival date highlighted in figures 6 and 7 are October 25, 2024 and June 11,

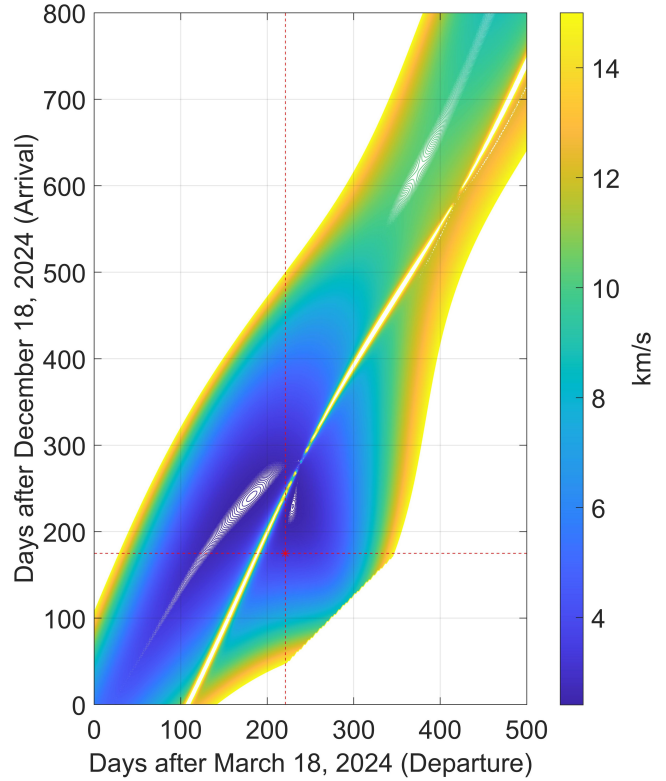


Fig. 7. Contours of arrival V_∞ for the 2024 Mars launch window

2025, respectively. For the dates previously mentioned, the spacecraft will have a departure C3 of approximately $20.5 \frac{\text{km}^2}{\text{s}^2}$, a hyperbolic excess velocity (V_∞) of approximately $3.29 \frac{\text{km}}{\text{s}}$, and a total transfer time of roughly 229 days. The planned transfer trajectory can be seen in Figure 8.

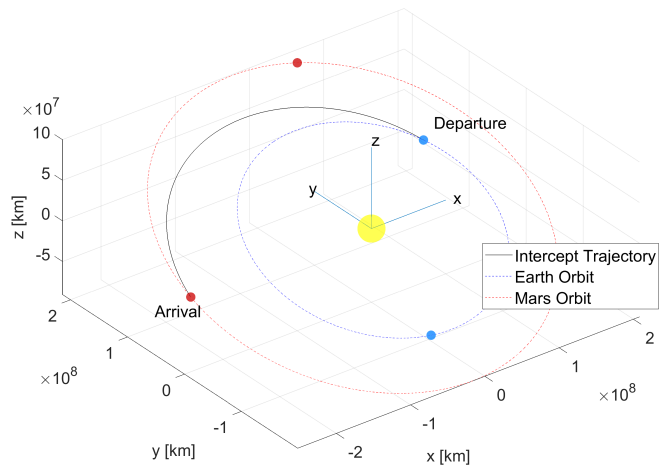


Fig. 8. Planned Mars transfer orbit viewed from a J2000 Sun-centered reference frame

During the cruise stage, small mid-course correction maneuvers can be performed to change how the spacecraft approaches Mars. If performed shortly after leaving Earth, the maneuvers can be incredibly small, on the order of

several $\frac{m}{s}$ ΔV . The corrections serve not only to maintain an accurate trajectory, but also to change the aiming radius (Δ) of the approach trajectory. The approximate values of the ΔV maneuvers can be seen in table X.

The primary function of adjusting Δ is to move the location of the periapsis of the transfer orbit at Mars. For AMERICA, Δ needs to be a value such that the periapsis is within Mars' atmosphere. If the periapsis is outside of Mars' atmosphere, the lander will effectively miss the planet and continue on a flyby trajectory. A periapsis roughly 24 km below the Martian surface has been chosen to ensure that the lander will intersect Mars' atmosphere. To achieve the desired periapsis, a Δ of approximately 6,163 km needs to be achieved through mid-course corrections.

Figure 9 shows the planned approach trajectory once the spacecraft has entered Mars' sphere of influence. The chosen periapsis of 24 km below the surface also determines the velocity the lander enters the atmosphere with (V_{atm}) and the flight path angle (γ) at which the lander enters the atmosphere. For the specified periapsis, the lander will enter the atmosphere with a V_{atm} of approximately $5.94 \frac{km}{s}$ and a γ of about 13° .

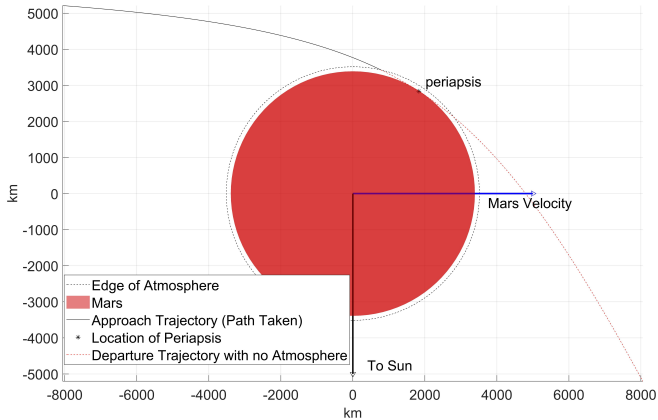


Fig. 9. AMERICA's approach trajectory to Mars with location of atmospheric intersection

Of additional importance to the mission is the first occurrence of the Mars solar conjunction after the mission has landed. The solar conjunction creates difficulties for communication to the vehicle on Mars due to interference caused by the Sun blocking direct line of sight to Mars. The vehicle lands on Mars on June 11, 2025. The first solar conjunction after landing on Mars will occur around January 2, 2026. Approximately 7 months will be available for the vehicle to start operations and collect data before being placed in an autonomous state for approximately 2 weeks around the time of the solar conjunction to be able to collect data without human intervention.

2) *Entry, Descent, and Landing (EDL)*: The entry, descent, and landing (EDL) phase will begin when the spacecraft reaches the Martian atmosphere, assumed to be at about 125 km above the surface, and ends with the lander safe on the surface of Mars approximately 7.5 minutes later. Prior to entry,

the spacecraft will jettison its cruise stage, and the remaining spacecraft is referred to as the entry vehicle, consisting of the aeroshell and lander. The EDL timeline was modeled using an exponential atmosphere, with a 700 kg entry vehicle mass, a $33.8 \frac{kg}{m^2}$ ballistic coefficient, a drag coefficient of 1.65 for the 70° sphere-cone, and a drag coefficient of 0.5 for the 19.7 m disk-band-gap Viking-legacy parachute [47]. This parachute, along with its deployment mortar, are stowed at the top of the back shell. The peak loading experienced right after parachute deployment is determined by multiplying the resultant drag-force by the opening force coefficient, which is 1.3 for the disk-band-gap parachute. The peak loading is approximately 21 kN. In addition, the entire trajectory is assumed to be two-dimensional. Pre-parachute analysis was performed using Allen-Eggers ballistic entry trajectory solution.

Knowing the results from the analysis on the spacecraft's astrodynamics, yielding the entry flight path angle and velocity, critical parameters are determined. Peak deceleration will occur at 40 km above the surface, with an approximate magnitude of 9.4 Earth g's. Figure 10 shows the descent of the lander.

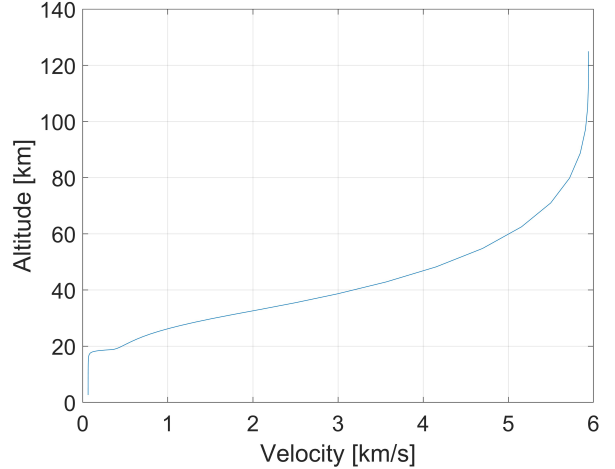


Fig. 10. Descent profile of entry vehicle, with parachute deployment occurring at approximately Mach 1.7 and reaching a terminal velocity of $63.5 \frac{m}{s}$

The parachute deploys about 165 seconds after entry, at an altitude of 18 km, and velocity around $410 \frac{m}{s}$, and heat shield separation occurs shortly after. Afterwards, the back shell, with the parachute attached, separates from the descent stage, at approximately 1.5 km above the ground, moving at a terminal velocity of $65.3 \frac{m}{s}$. At this point, the retrorockets on the descent stage begin firing, starting the powered descent phase. After the engines have decelerated the descent stage sufficiently, it maintains that velocity. The descent stage at this point will lower the lander on a bridle, in a sky-crane maneuver. There will also be a non-negligible horizontal distance traversed by the spacecraft across the entire entry, descent, and landing, caused by the non-horizontal entry angle. In total, the spacecraft travels about 558 km laterally from its initial entry point.

3) *Thermal Protection System (TPS)*: In order to ensure the lander and corresponding science payload arrive safely on the Martian surface, it is integral that a thermal protection system is utilized in the spacecraft's entry and descent. This will consist of an ablative heat shield that will absorb the bulk of the heat produced during entry. This was modeled using the Sutton-Graves equations for peak heat rate and total integrated heat load. These are further simplified for an analytical estimate with the analytic solution to the Allen-Eggers equations. The heat rate and heat load were determined using an entry velocity of $5.94 \frac{km}{s}$, flight path angle of 13° , and ballistic coefficient of $33.8 \frac{kg}{m^2}$. This solution assumed a nose radius of 0.6625 m [48]. The peak heat rate is calculated to be $54.73 \frac{W}{cm^2}$. The total heat load is $4009.6 \frac{J}{cm^2}$. These estimates influenced the selection of the heat shield material. If the entry mass of the spacecraft is assumed to be 700 kg , the estimated heat shield mass is calculated to be 63.48 kg . The corresponding backshell mass would be 98 kg . The appropriate heat shield material was determined to be Phenolic Impregnated Carbon Ablator (PICA). The corresponding required material thickness was calculated to be approximately 3.61 cm .

4) *Propulsion*: In order to ensure the spacecraft maintains its trajectory to Mars and create a propulsive descent to the martian surface, the AMERICA spacecraft contains two independent propulsion systems. A cold gas system and a system for powered descent onto the Martian surface.

During the cruise phase as shown in figure 11 the spacecraft may need to make 5-6 trajectory adjustments to ensure its proper and timely arrival to Mars. These trajectory adjustments require the spacecraft to make a total of $30 \frac{m}{s} \Delta V$ adjustments. Trajectory changes are done by a cold gas propulsion system which requires 36.06 kg of N_2 , two Northrop Grumman 80148-1 Tanks, four check valves, and eight Moog 058-1 cold gas thrusters.

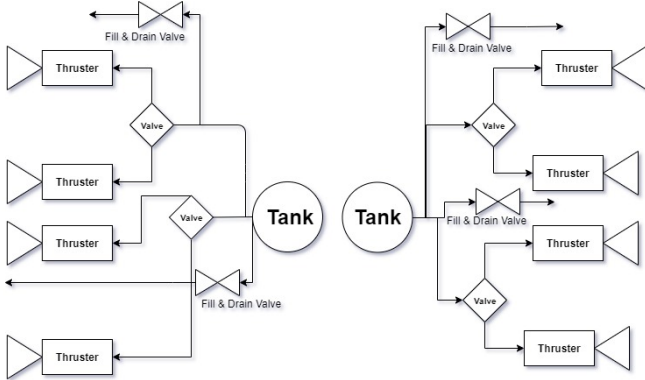


Fig. 11. Propulsion schematic for cruise stage using N_2 and having $30 \frac{m}{s}$ for trajectory changes

Figure 12 depicts the propulsion system needed for the powered descent onto the Martian surface, which is done by a powered descent of a sky crane. The ΔV of the powered descent is $403.3 \frac{m}{s}$ while the sky crane process has a ΔV of $199.59 \frac{m}{s}$. The sky crane will hover 20 m above the ground

TABLE X
CRUISE STAGE OVERVIEW

Property	Value
ΔV	$30 \frac{m}{s}$
Thruster	Moog 058-118 (8x)
Thruster Mass	23 g each [33]
Thruster Material	Stainless Steel, Nylon [33]
Thruster ISP	57 sec [33]
Nominal Thrust	3.6 N @ 15.7 bar [33]
Tank	Northrop Grumman 80148-1 (2x) [34]
Tank Weight	1.59 kg [34]
Tank Material	Titanium [34]
Tank Volume	18.03 L [34]
Propellant	36.06 kg of N_2

for 30 seconds and fly to a safe distance away. The landing propulsion system requires 49.269 L of hydrazine (H_2N_4) for the powered descent and 8.3 L of propellant for the skycrane to hover and fly off. Along with the hydrazine propellant, 132.74 L of helium is needed as a pressurant. The Aerojet Rocketdyne MR-104H engines are used and each provide 510 N of thrust. With eight engines, 4080 N of thrust is generated to slow down the spacecraft. In order to store the propellant, two Northrop Grumman 8018-1 tanks are utilized while a single Northrop Grumman 80326-1 tank is used to hold the pressurant. Two fill and drain valves are also present in the system in order to allow pressurant and propellant to release. A latch valve is present to open the thrusters to start catalyzing the propellant and a pressure sensor to indicate the pressure of the propellant passing through.

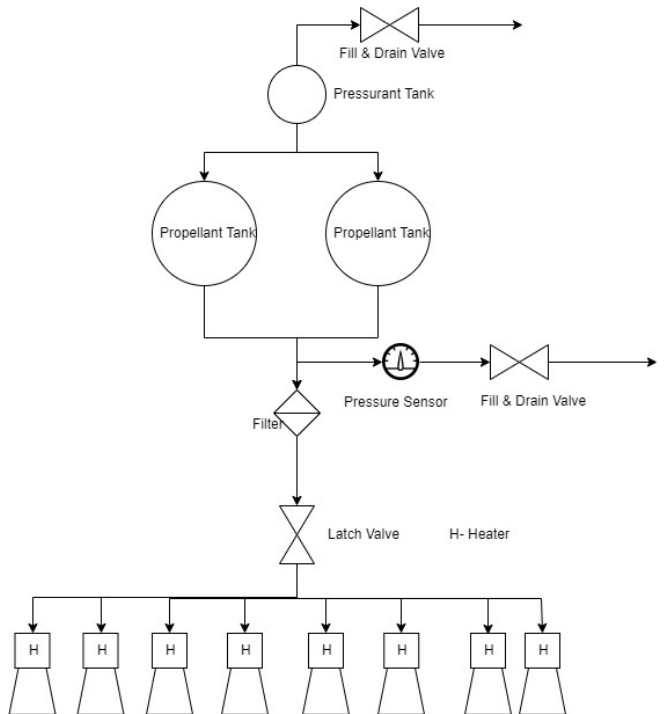


Fig. 12. Propulsion schematic for landing stage using hydrazine as a propellant and helium as a pressurant for the skycrane and powered decent procedure and executing ΔV s of $199.59 \frac{m}{s}$ and $403.31 \frac{m}{s}$ respectively

TABLE XI
LANDING STAGE OVERVIEW

Property	Value
ΔV Propulsive Descent	403.31 $\frac{m}{s}$
ΔV Sky Crane Procedure	199.59 $\frac{m}{s}$
Thruster	Aerojet Rocketdyne MR-104H (8x)
Thruster Mass	2.4 kg each [35]
Thruster Material	Stainless Steel, Nylon [35]
Thruster ISP	237 sec [35]
Nominal Thrust	510 N [35]
Propellant Tank	Northrup Grumman 80186-1 (2x) [36]
Propellant Tank Weight	23.20 kg each [36]
Propellant Tank Material	Titanium [36]
Propellant Tank Volume	28.7 L each [36]
Total Propellant	57.4 kg of H_2N_4
Pressurant Tank	Northrop Grumman 80458-1 [37]
Pressurant Tank Weight	20.41 kg [37]
Pressurant Tank Material	Titanium [37]
Pressurant Tank Volume	132.74 L [37]
Total Pressurant	132.74 kg of helium

5) *Attitude Determination and Control System (ADCS):* AMERICA is a three axis stabilized spacecraft. The eight cold gas thrusters covered in section III-A4 will be used to control AMERICA's orientation during cruise stage.

To measure the changes orientation during the cruise and landing stage, AMERICA will be equipped with an inertial measurement unit (IMU). IMUs consist of an accelerometer and gyroscope to keep track of the orientation of the spacecraft over a short amount of time. For the landing stage, the Honeywell MIMS [38] IMU will be used. In addition, MIMS has a long flight heritage for deep space flight.

TABLE XII
HONEYWELL MIMS IMU [38]

Property	Value
Mass	4.2 kg
Volume	20 cm d x 13.2 cm h
Power	2.5 W
Supply Voltage	28 VDC
Rotation Rate	$\pm 375 \frac{\deg}{s}$
Survival Temperature	-30°C to +70°C
Gyro Bias (1 σ)	$\leq 0.005 \frac{\deg}{hr}$

Mounted on the cruise stage, two Ball CT2020 [39] star trackers will measure the orientation of the spacecraft by taking an image, then comparing the stars in that image to a database of known locations of stars.

TABLE XIII
BALL CT2020 [68]

Property	Value
Mass	3 kg
Volume	10 cm x 10 cm x 40 cm
Power	3.35 W
Supply Voltage	5 VDC
FOV	25° Circular
Accuracy	1 arcsec

In order to prevent the overloading of charge-coupled device array in the CT2020 star trackers, six Bradford Coarse Sun Sensors will be used to provide the orientation information

to ensure neither is pointed at the sun. The sun sensors are pointed in groups of three opposite each group pointing direction so the sun is always visible.

TABLE XIV
BRADFORD COARSE SUN SENSOR [67]

Property	Value
Mass	0.215 kg
Volume	11 cm x 11 cm x 30 cm
Power	28 W
Supply Voltage	5 VDC
FOV	$\pm 90^\circ$ Hemisphere
Accuracy	1°

B. Thermal Control System

During the cruise stage, the thermal environment calculations were made assuming a spacecraft absorptivity of 0.23, an emissivity of 0.85 using white paint (S13G-LO) at a point near the Earth sphere of influence and at a point near the Mars sphere of influence. The spacecraft will face minimum temperatures of -62° C near Mars and a high temperature of 44° C near Earth. Passive thermal control systems will be primarily used, including a 15 layer multi-layer insulation (MLI), a 10 panel thermal radiator, looped heat pipes, and two light weight radioisotope heating units (LWRHU) to be positioned around the warm electronics box (WEB) outlined later in the section [44].

TABLE XV
LWRHU SPECIFICATIONS [44]

Property	Value
Mass	40 g
Volume	Length: 3.2 m Diameter 2.6 m
Power Generated	1.2 W

The MLI is to be included on structural members exposed to space, antennas, the thermal radiator, and the solar arrays [43]. There will be looped heat pipes running through all the key components of the spacecraft, including the WEB, inside which are the batteries, communication and data handling hardware, and all spacecraft computers.

The WEB will be kept within the limits of 0° C and 40° C to accommodate the most sensitive limits of the components inside, with a 20° C buffer. This will be accomplished through the spacecraft's heat rejection system (HRS), comprised of the looped heat pipes, which will take excess heat to the radiator to be expelled. The radiator will be autonomously operated through the use of heat switches and louvers to determine how much heat needs to be expelled in order to keep the WEB within operating temperatures [45].

In case of a need to generate heat, specifically in the lander phase of the mission, the spacecraft will be equipped with electrical heaters placed in strategic locations near the WEB and other scientific equipment.

The lander stage of the mission will impose specific requirements on the thermal control system based on what scientific equipment will need to be active for a particular mission. To

TABLE XVI
WEB COMPONENTS [44]

Component	Operating Temperature (° C)
Batteries	-20 to 60
Computers	-25 to 75
C&DH	-55 to 70
IMU	-30 to 70
TCXO	-40 to 85

satisfy these needs, the looped heat pipes will be utilized to move heat from the electrical heaters to the necessary locations.

The electrical heaters will remain off during standby and the lander will rely on RHUs to keep above minimum temperature values. If the RHUs fail to keep the components above the threshold, the electrical heaters will be activated by a heat switch. The night time temperature on Mars can reach as low as -100° C, and with this in mind the constant heat from the LWRHUs will keep the lander's most demanding components much closer to operating temperatures during the night, allowing for quicker warm up and more time on mission.

C. Mechanical Design

The major design constraints for the lander are to ensure that all science equipment can function properly and that the lander can survive and perform its tasks as designed in a hostile Martian environment. Additional constraints include cost of materials and the ability to construct the lander before scheduled deadlines. The lander will be able to obtain Martian samples and deposit them in scientific instruments on board so that the samples are able to be analyzed. To accomplish this, a robotic arm with a scoop will be used. In addition to providing samples for the SAM unit, the robotic arm will also include a ChemCam.

The SAM unit will be loaded with soil samples from the robotic arm. The input for this instrument is located at the top of the unit. This requires the arm to be able to take samples at the proper depth as well as transport them to the intake. To accomplish this, the robotic arm will have a scoop mounted to the end of the arm that will be able to dig in to the surface and transport soil samples. The TECP will be mounted on the end of the robotic arm so that it can make contact with the soil and perform its data collection. Because several different operations need to happen on the robotic arm, it will be able to switch between which instrument is being used at any given time. The last major consideration for the robotic arm is the ChemCam. The ChemCam requires an input of dust from the side of the instrument. The robotic arm will be able to gather dust and properly insert it into the instrument.

1) *Cruise Stage and Entry Vehicle:* During the transit stage, the main design considerations are the location of thrusters, antennas, and solar panels. The solar panels will be able to rotate to constantly face the sun during transit. The dipole antennas are mounted opposite the heat shielding at an angle of 120° relation to each other. The thrusters are positioned orthogonal to the extended solar panels.

The cruise stage has a maximum diameter of 2 meters. The heat shielding is a 70° cone with a spherical tip. The shielding behind the heat shield starts at 2 meters and then tapers to 0.8 meters at 45°. The internal volume for the lander is 12.5 m³.

When the transit stage is preparing for entry unnecessary equipment for landing will be jettisoned, such as solar panels. The entry stage only consists of equipment and sensors needed for a safe landing.

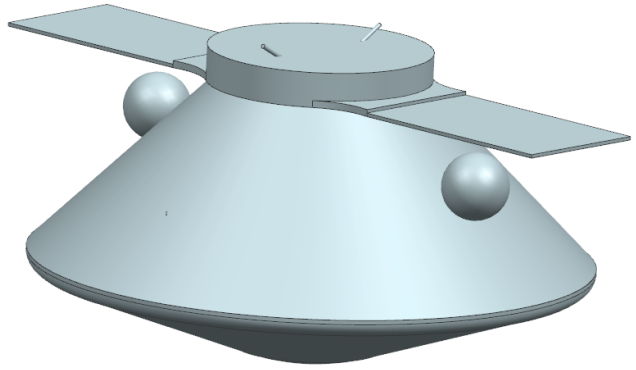


Fig. 13. Cruise stage

2) *Sky Crane:* In order to ensure that the scientific instruments aboard the lander can collect reliable readings and data, there is a need to disturb the surface around the landing site as little as possible. To accomplish this, the mission will utilize a sky crane to slowly and gently lower the lander to the surface. The AMERICA sky crane's configuration and design, as shown in [14], is a modified model of the MSL skycrane [73]. Some differences include longer tethers so as to better preserve the landing site, fewer thrusters for the smaller lander, and smaller propellant tanks as the AMERICA lander has a lower mass than the Curiosity Rover.

Once the descent stage is separated from the back shell and parachute, the thrusters fire to slow the lander. This continues until the lander detects that it is about 40 m above the surface. At this point, pyros are fired and the lander is separated from the sky crane except for the bridle: three 9 m nylon tethers which are attached to the lander near its center of mass. Additionally, an umbilical cord remains attached to lander to power it during its descent.

The lander descends at around 0.5 $\frac{m}{s}$ until the lander detects contact with the martian surface. After a two-second delay to ensure good contact, pyro cutters on the lander are fired and the bridle is severed. The nylon tethers automatically rewind to the sky cranes spool on a spring system. The sky crane then flies at least 600 m away before crashing into the surface.

3) *Lander:* The primary structure for the lander consists of an irregular octagonal deck supported by three titanium landing legs and six support struts. The deck area is 1.43 square meters with the longest sides at 0.88 m, and the shortest at 0.51 m, allowing plenty of space for the lander's scientific

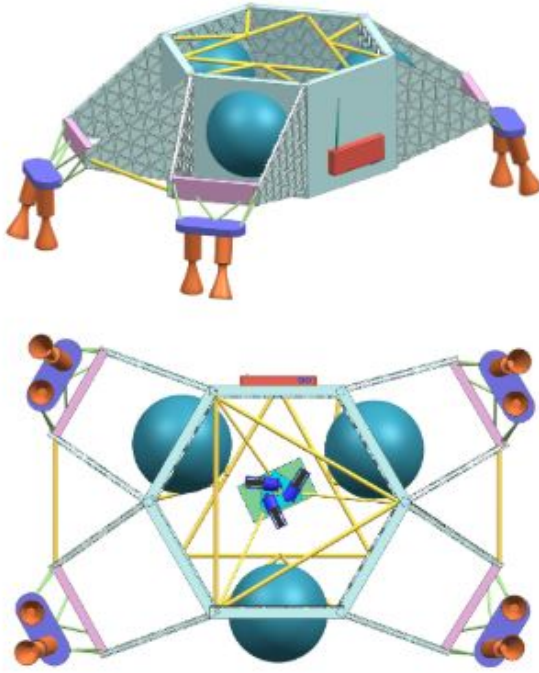


Fig. 14. Sky Crane isometric and bottom views

payload while fitting within the 2 meter diameter of the cruise stage. The deck will rest between 0.9 – 1.22 meters above the surface, depending on the composition of the regolith and the landing site. With the solar panels fully deployed, the maximum wingspan of the lander is 5.25 meters.

The mass distribution of the lander (see table XVII) is based around the heaviest components it carries: the SAM Unit, the Mastcam-Z, the Comms System, and the solar array. Figure 16 shows the layout of the deck and major scientific and mechanical subsystems. The lander's avionics and some of its communications and other subsystems are mounted to a thermally protected component deck on the underside of the main deck. Due to the use of a sky crane, there are no thrusters nor propellant tanks on the lander. Furthermore, the legs of the lander are not designed to compress with the shocks of the landing as it is not necessary.

TABLE XVII
LANDER MASS DISTRIBUTION

Part	Mass
Scientific Payload	59 kg
Primary Structures	154 kg
Secondary Structures	78 kg
Robotic Arm	10 kg
Solar Array	19 kg
Comms System	75 kg
Total	396 kg

The lander's solar panels extend from the longest sides of the deck directly opposite to one another to balance any moments they create. The SAM unit, one of the heaviest subsystems on the lander, is placed on the opposite side of the deck as the Mastcam-Z, with the majority of the comms subsystems also placed across from the SAM unit to ensure

that the center of gravity of the lander is as close to the center of the lander structure as possible. The remaining scientific instruments are placed opposite the Robotic Arm such that, even when the arm is fully extended, the lander does not tip and all three landing legs remain in contact with the surface at all times.

The lander has several operational states. For transit, the lander remains in its stowed configuration (see figure 17) with the 3 landing legs folded underneath of the main component decks. The solar panels are in their folded configuration. All of the scientific payloads are also stowed. After the heat shields are jettisoned, the legs are extended. The solar panels, robotic arms, and MastCam-Z may be re-stowed at any time during the mission, but the legs cannot.

The legs of the lander are to be made of titanium for its high strength-to-weight ratio. The majority of the secondary structures are to be constructed of aluminum.

4) Robotic Arm: The robotic arm was designed to have five degrees of freedom. The degrees of freedom are shown in figure 18.

There are a total of five degrees of freedom of the robotic arm and two metal lengths. These degrees of freedom serve to allow the arm to rotate and tilt at the base. There is one degree of freedom between the two lengths and two degrees of freedom at the end to control the scoop. The lengths of the robotic were designed to be able to reach the maximum area while staying under 10 kg. The two lengths of the robotic arm has a length of 1.463 meters and a radius of 0.02 meters. The total area that the arm is able to sample from is 7.2 m^2 . The sampling area is shown in figure 19.

The inner radius of the sample area is 0.522 meters and outer radius of 2.4 meters. The sample area encompasses 150 degrees.

D. Communications

1) Overview: The communications subsystem will receive commands from Earth via NASA's Deep Space Network (DSN), and relay science and engineering data back to Earth for analysis. Engineering data and commands will be sent primarily directly to and from the 34 m DSN antennas using the X band during the cruise stage. Due to the large volume of science data generated, science data will be communicated by an Ultra High Frequency (UHF) transmission system to the Mars Relay Network, a collection of transponder payloads located on several Mars orbiters. By using the network, the lander does not need a high gain antenna, greatly reducing the required mass of the communication system. Once the spacecraft has landed on Mars, command and telemetry data will also be routed through the network.

2) Hardware: Figure 23 shows a block diagram schematic for the X band and UHF band communication systems. Each system uses redundant, cross linked components, increasing the overall communication system's reliability.

Both systems consist of similar components. A pair of transponders process the received signals and modulate the

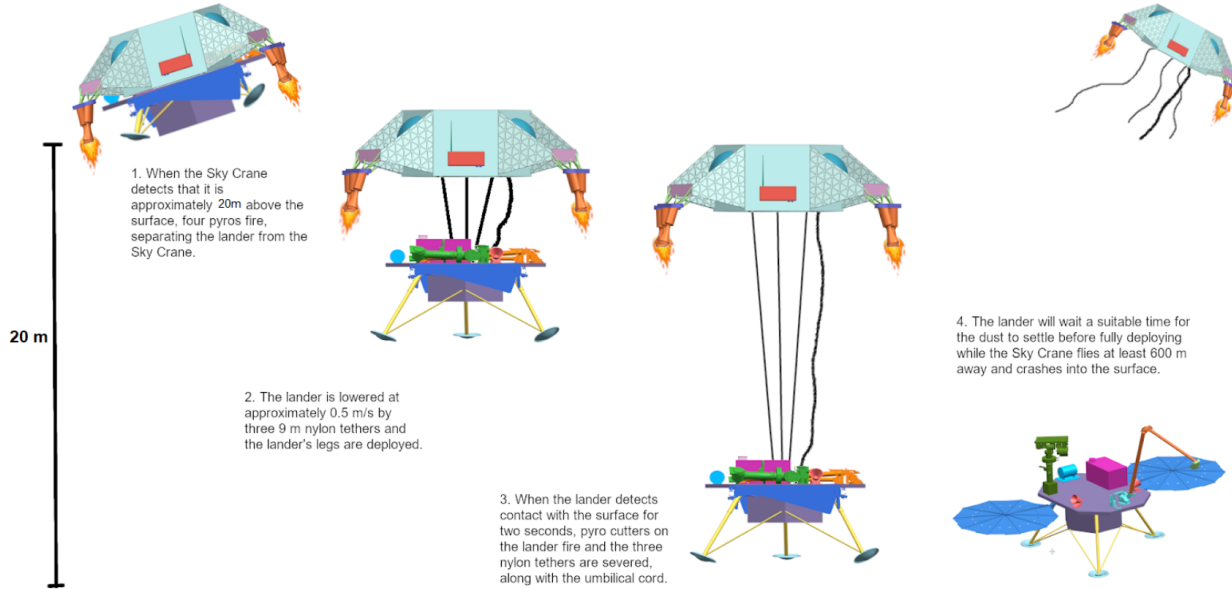


Fig. 15. AMERICA skycrane concept of operations

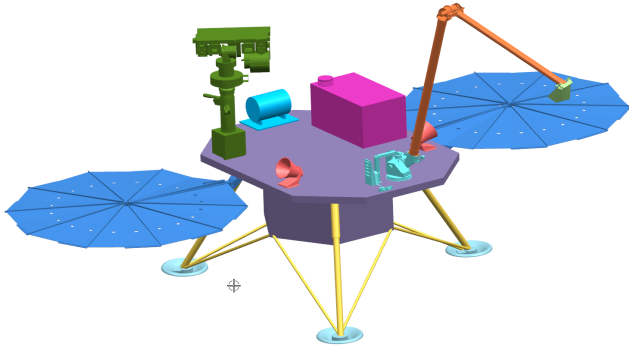


Fig. 16. Lander in deployed configuration [70] [71] [72]

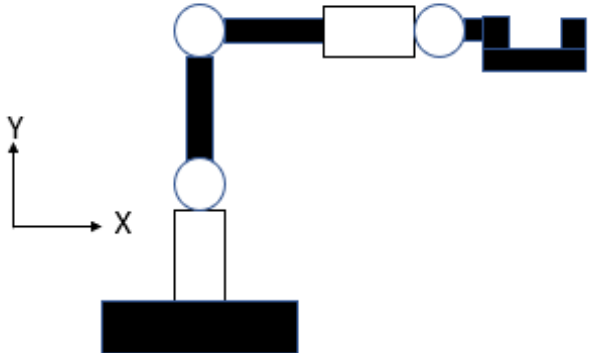


Fig. 18. Schematic of the robotic arm from a side view. White cylinders represent joints and black rectangles are lengths of the arm

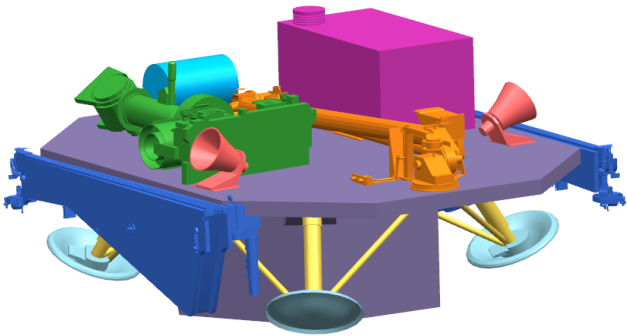


Fig. 17. Lander in stowed configuration

carrier signal. All transmitted and received signals use Binary Phase Shift Keying (BPSK) modulated $k = 7$, $r = \frac{1}{2}$ convolutional encoding, the standard for deep space communication [50]. The X Band system uses two General Dynamics Small Deep Space Transponders (SDSTs), while the UHF band

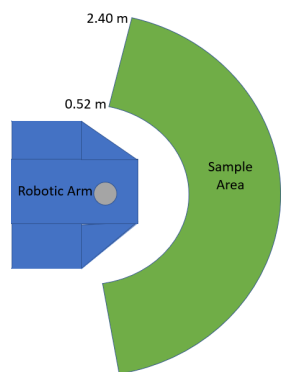


Fig. 19. Sampling area of robotic arm

system uses two Electra-Lite UHF Transponders.

To receive an uplink, one of the RF switches shown in figure 23 is used to select an antenna. The output of the selected antenna is fed to a diplexer, which is used to separate uplink and downlink frequencies. The uplink signal is then passed through a bandpass filter in order to isolate the appropriate frequencies. The uplink and downlink frequency bands for both systems are shown in table XVIII. The exact carrier uplink frequency within this band will be selected after consulting the JPL Frequency Manager [64].

TABLE XVIII
UPLINK AND DOWNLINK FREQUENCY BANDS FOR THE UHF AND X BAND COMMUNICATION SYSTEMS

System	Uplink (MHz)	Downlink (MHz)	Subcarrier (kHz)
X band	7145 - 7190 [51]	8400 - 8450 [51]	16 [50]
UHF	435 - 450 [56]	390 - 405 [56]	-

The uplink signal is then processed by the appropriate transponder and sent to the Command and Data Handling (C&DH) subsystem.

To initiate a downlink, the spacecraft uses the relevant transponder to encode the data on a carrier within the frequency range specified by table XVIII. Again, the exact frequencies used will be chosen after discussion with the JPL Frequency Manager [64]. These carriers are generated in phase with the received uplink signal, if there is one. Otherwise, they are generated in phase with the ultra-stable oscillator (USO).

The X Band signal is then amplified by one of two General Dynamics Solid State Power Amplifiers (SSPAs) to a transmission power of 17 W [52]. The UHF system does not require an amplifier to achieve an adequate signal power.

In both systems, the output is sent through a polarizer to give the wave a right circular polarization that can be received by the ground and relay antennas [50][58]. The polarized output signal is then transmitted via the antenna selected by appropriate RF switch.

3) *Critical Event Telemetry and Solar Conjunction:* Critical events for this mission will use a link between the relevant X band antenna and a DSN 70 m antenna. During orbital insertion, the spacecraft will use the cruise stage Low Gain Antennas (LGAs), with the Medium Gain Antennas (MGAs) used as needed. The lander X band horn antennas will be used during the entry, descent, and landing (EDL) stage.

During solar conjunction, the spacecraft will be unable to receive commands from Earth, and data will be downlinked at a lower rate [66]. The first conjunction during the AMERICA mission occurs in January of 2026. This date occurs after EDL, and so will not interfere with any critical events. Prior to conjunction, the spacecraft will be sent commands to execute during the conjunction in order to continue the science mission. Data collection during this period will be reduced in order to accommodate lower downlink rates.

4) *Link Budgets:* Complete link budgets for several example links are shown in table XXI. The sample link budgets shown are representative of the average channel parameters

for each of the types of antennas that the AMERICA mission will communicate with. Table XXI shows a simplified link budget for each of the other communication links used during the mission. The path losses for all links were calculated at the maximum path distance for each link in order to determine a worst-case Eb/N0. For the cruise stage links, a path length of 266,000,000 km, the calculated maximum distance of the AMERICA spacecraft from Earth at any point during the cruise stage, was used. X Band links between the lander stage and the DSN used a path length of 400,000,000 km, the maximum distance between Mars and Earth [57]. Links between the lander UHF antennas and the Mars Relay Network antennas used the apoapsis of each orbiter, as given in [58], as the maximum path length.

Additional losses are those minor sources of loss inherent in the system, such as cable losses and antenna efficiencies. System noise temperature was calculated using the equation

$$T_s = \frac{T_a}{L_c} + \frac{T_t(L_c - 1)}{L_c} + T_0(F - 1) \quad (1)$$

[55, eqn. 9.48], where T_s is the system noise temperature, T_a is the effective antenna temperature, L_c is the passive component losses, T_t is the cable temperature, T_0 is a reference temperature, taken to be 290 K [53], and F is the noise figure of the system. The noise power (in dB), was calculated using the equation

$$P_{noise} = 10\log(kT_sB) \quad (2)$$

[53] where k is Boltzmann's constant, B is the equivalent bandwidth of the signal, T_s is the system noise temperature, and P_{noise} , is noise power in dB.

a) *Cruise Stage Antennas:* During the majority of the cruise stage, the AMERICA spacecraft will communicate with the 34 m Deep Space Network antennas using two X Band half wave dipole Low Gain Antennas (LGAs) of length 0.208 m. These antennas are mounted on the cruise stage and connected to the lander hardware via an umbilical, and will provide a gain of 1.6 dB [53] with an assumed efficiency of 70% [54]. Table XXI shows the link budgets for cruise stage communication with the 34 m Beam Waveguide (BWG) DSN antenna. Both the 34 m BWG and High Efficiency (HEF) DSN antennas allow for a worst case uplink rate of 32 bits per second (bps), and a single tone downlink signal with the LGAs. This single tone signal will be used to provide spacecraft tracking, and as a simple indicator of spacecraft health.

The downlink signal to the 70 m DSN Antenna from the Cruise stage LGAs is still too low to send data over, but offers an improved carrier signal to noise ratio (SNR) for the single tone.

When the SNR of the LGAs has too low a noise margin because the spacecraft is far from Earth, communication will occur as necessary using two gimballed X band medium gain (MGA) horn antennas with a diameter of 0.184 m and a gain of 20 dB [53]. The horn antenna efficiency is assumed to be 60% [55]. These horn antennas are also connected to the lander stage using an umbilical. The horn antennas allow for a higher uplink data rate, but pointing requirements mean that the LGAs will be used whenever possible. During normal operations, the

MGAs will still provide a single tone downlink, but during critical events, the MGAs can be used to provide up to 64 bps downlink to a 70 m antenna.

b) Lander X Band Antennas: The AMERICA lander uses two gimballed X band horn antennas to receive commands and send engineering data to and from Earth. These horn antennas, with a diameter of 0.184 m, provide a gain of 20 dB [53]. The horn antenna efficiency is assumed to be 60% [55]. Similar to the cruise stage, the 34 m BWG and HEF antennas will be used for daily operations, and the 70 m antennas will be used for critical event coverage, primarily EDL stage. Table XXI shows a representative link budget between the 34 m BWG antennas and the lander X band horn antenna. As shown in tables XXI and XXII, the X Band lander antennas provide a higher uplink data rate than the cruise stage LGAs, allowing a consistent command uplink from Earth if needed. At the maximum Earth-Mars distance, the lander X band antennas can only provide a single tone downlink to the DSN, due to the DSN's minimum downlink bit rate of 40 bps [50], but at distances of closer than 370,000,000 km, the lander X band antennas can provide a downlink rate of 64 bps at an Eb/N0 of 7.8 dB. This communications limitation is overcome by using the UHF band link with the Mars Relay Network for primary operations.

c) Lander UHF Antennas: Once the lander is on the surface of Mars, science data will be relayed to Earth through the Mars Relay Network. The Relay Network consists of UHF transponder payloads on the Mars Odyssey Orbiter, the Martian Atmosphere and Volatile Evolution (MAVEN) Orbiter, the Mars Reconnaissance Orbiter (MRO), and the ExoMars Trace Gas Orbiter (TGO) [58]. The AMERICA lander will communicate primarily with MRO via an Electra-Lite UHF transponder and a pair of gimballed helical antennas. The helical antennas have a diameter of 0.590 m and a length of 1m, providing 20 dB of gain [53] with an assumed efficiency of 60% [53]. The link budgets for communication with MRO are given as an example in table XXI, and the data rates with the other orbiters are shown in table XXII. The UHF links, due to the proximity of the relay orbiters, provide data rates several orders of magnitude larger than the direct links to Earth.

5) Tracking Telemetry: During the cruise stage, spacecraft positioning and velocity data will be obtained by using the Deep Space Network's Coherent Doppler Data tracking service, as well as the Delta-Differential One-way Ranging (Delta-DOR) tracking service. The Doppler tracking service requires a tone SNR of >15 dB for the uplink signal, and >10 dB for the downlink signal [50], and the Delta-DOR services requires a SNR of >18 dB [50]. As shown in tables XXI and XXII, the required Doppler SNR is achievable throughout the cruise stage, using either an LGA or an MGA. The Delta-DOR required SNR is achievable using the MGA throughout the cruise stage. Tables XIX and XX show the schedule for tracking throughout the cruise stage, and is based off of the tracking plan for the Phoenix mission [65]. Critical periods of tracking are shortly after launch, about two months before entry into the Mars atmosphere, and the week around each trajectory correction maneuver (TCM).

TABLE XIX
COHERENT DOPPLER DATA TRACKING SERVICE SCHEDULE

Start Time (Days)	End Time (Days)	Weekly Contacts	Contact Duration (hours)
Launch	Launch + 14	14	12
Launch + 15	Entry - 57	3	8
TCM - 3	TCM + 4	14	12
Entry - 56	Entry	14	12

TABLE XX
DELTA-DOR TRACKING SERVICES SCHEDULE

Start Time (Days)	End Time (Days)	Weekly Contacts	Contact Duration (hours)
Launch + 36	Launch + 42	7	2
Entry - 56	Entry - 14	3	2
Entry - 14	Entry	21	2
Other time periods		1	2

E. Command and Data Handling (C&DH)

1) Data Collection & Uplink Schedule: Communications capabilities represent the limiting factor in determining reasonable data collection rates for the scientific instruments onboard the lander. Access periods and data rates from the Mars orbiters to the deep space network are well defined. However, access between the lander and orbiters for communications relay is geometry dependent. An assessment of typical access windows over the course of a martian year was performed to determine maximum ideal data downlink capability.

The Mars Reconnaissance Orbiter, Mars Odyssey, MAVEN, and the Trace Gas Orbiter (TGO) are the satellites in Mars orbit capable of communications relay from the lander to the DSN. The orbits of these relay satellites at a given epoch are drawn about Mars with the proposed landing site in the MFF highlighted in figure 20.

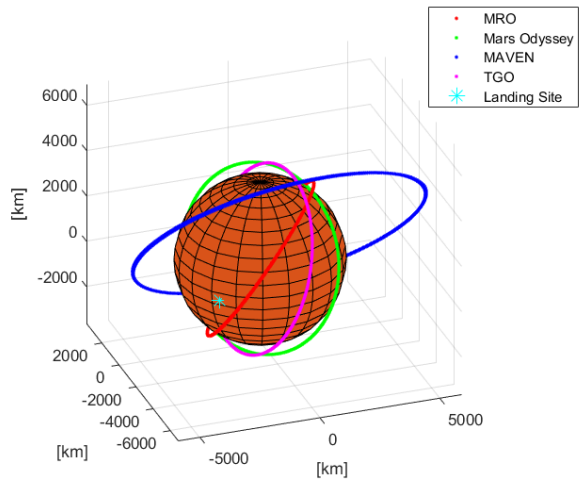


Fig. 20. Orbits of the satellites used as communication relays

Based on these orbital conditions for the relay satellites, figure 21 shows line of sight periods from the lander to each orbiter. For each access period and each orbiter, the expected (worst case) usable downlink data rates were used to determine

TABLE XXI
EXAMPLE LINK BUDGETS FOR COMMUNICATION LINKS WITH EACH AMERICA ANTENNA¹

Spacecraft Antenna Ground/relay Antenna	Cruise Stage X band 34 m BWG DSN		Lander Stage X band 34 m BWG DSN		Lander UHF MRO UHF	
Link Property	Uplink Values	Downlink Values	Uplink Values	Downlink Values	Uplink Values	Downlink Values
Carrier Frequency (MHz)	7145-7190 [51]	8400-8450 [51]	7145-7190 [51]	8400-8450 [51]	435-450 [58]	390-405 [58]
Subcarrier Frequency (kHz)	16 [50]	16 [49]	16 [50]	16 [49]	N/A	N/A
Transmitter EIRP (dBW)	110 [50]	12.3 (17 W) [52]	110 [50]	12.3 (17 W) [52]	7.0 (5 W) [58]	9.29 (8.5 W) [56]
Transmitting antenna gain (dB)	0 dB [50]	1.6 [53]	0 dB [50]	20 [53]	2.9 dB [58]	20 [53]
Space loss (dB)	-278.1 [53]	-279.5 [53]	-281.6 [57][53]	-283 [57][53]	-156.6 [58][53]	-155.6 [58][53]
Total atmospheric loss (dB)	-0.2 [55]	-0.2 [55]	-1.35	-1.35	-0.5 [57]	-0.5 [57]
Additional losses (dB)	-1.3	-2.9	-1.3	-3.5	-1.32	-3.6
Receiver antenna gain (dB)	1.6 [53]	68.2 [50]	20 [53]	68.2 [50]	20 [53]	2.9 [58]
Received power (dBW)	-168	-200.4	-154.3	-187.3	-128.5	-127.6
Bandwidth (Hz)	64	2	1024	2	256000	256000
Noise Power (dBW)	-184.3	-212.6	-173	-212.6	-146.7	-146.4
Eb/N0 (dB)	16.4	12.2	18.8	25.2	18.2	18.8
Data rate (bps)	32	Single tone	512	Single tone	128000	128000

TABLE XXII
DATA RATES AND EB/N0 FOR LINKS NOT SHOWN IN TABLE XXI

Spacecraft Antenna	Ground/Relay Antenna	Uplink Data Rate (bps)	Eb/N0 (dB)	Downlink Data Rate (bps)	Eb/N0 (dB)
Cruise Stage LGA	DSN 34 m HEF	32	16.4	Single tone	12.3
Cruise Stage LGA	DSN 70 m	128	16.3	Single tone	18.5
Cruise Stage MGA	DSN 34 m BWG	2048	16.7	Single tone	30.6
Cruise Stage MGA	DSN 34 m HEF	2048	16.7	Single tone	30.7
Cruise Stage MGA	DSN 70 m	8192	16.7	64	18.8
Lander X Band	DSN 34 m HEF	512	18.8	Single Tone	25.2
Lander X Band	DSN 70 m	2048	18.7	128	10.4
Lander UFH	Mars Odyssey	256000	17.2	128000	17.7
Lander UHF	MAVEN	128000	17.6	64000	19.1
Lander UHF	TGO	128000	17.6	512000	16.6

the volume of data the lander will be capable of sending (a similar method was used to assess uplink capabilities as well.) MAVEN's elliptical orbit causes line-of-sight windows to vary substantially over time, which causes variation in communications capability during different periods in the mission. It is desired that communications capability is consistent over time, so orbiters with orbits of lower eccentricity are preferred.

Since Mars' oblateness is approximately twice that of Earth's, it is necessary to examine the impact of precession on these orbits and on the access intervals and data transfer capability. Figure 22 shows total downlink data transfer volume per sol as a function of time over the course of a martian year. As the satellites precess in their orbits, data transfer volume per day changes fairly significantly (primarily due to the high eccentricity of MAVEN's orbit.) A similar trend follows for uplink, though the magnitude of data capacity is different.

Over an average sol, using all of the orbiters for communications yields a 325 MB data transfer volume, which gives a weekly data transfer cap of 2.275 GB. A reasonable science data collection schedule only requires 300-400 MB per week downlink, so it is possible to only use a subset of these orbiters to meet this demand. Considering only MRO, the weekly downlink capability from the rover to the orbiter is only 188 MB. Therefore, one of two communication opportunities with TGO will also be used per sol, which brings the total weekly downlink capability from the lander to the orbiters to 584 MB, exceeding the budget of 300-400 MB per week required to send science data back to Earth. By using only MRO and TGO for communications relay, it becomes possible to expect consistent non-time-varied communications capability over the course of the mission since the orbits are both circular.

With a sufficient data throughput capability to the orbiters,

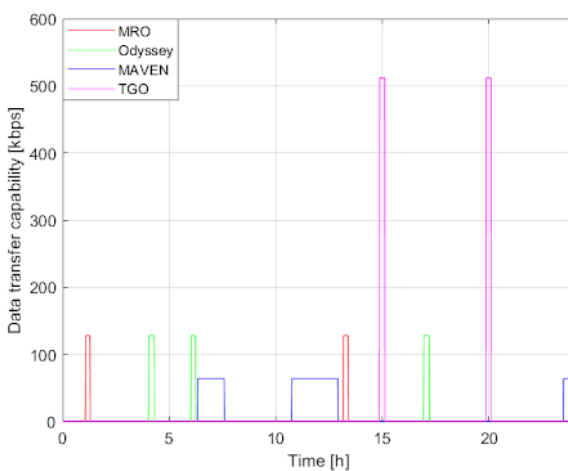


Fig. 21. Data downlink per orbiter over one sol

¹The DSN transmitter power given is the Effective Isotropic Radiated Power (EIRP), which includes the antenna gain, so the transmitting antenna gain is listed as 0 dB

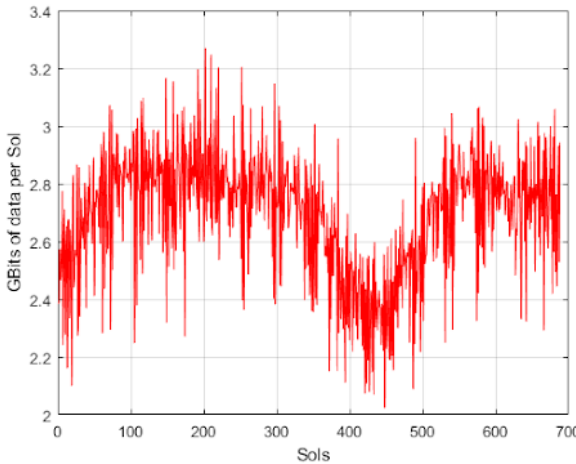


Fig. 22. Data downlink transfer volume per sol over a typical martian year

it is prudent to also determine data transfer limitations from the orbiters to the DSN. MRO has an estimated 84 hours of contact capability with the DSN per week. The orbiter's memory is limited, and there will be other surface missions collecting data on Mars during the proposed mission (Mars 2020, Curiosity, ExoMars 2020, HX-1), so a conservative estimate preserves 5% of MRO's memory and communications budget for AMERICA uplink/downlink. With MRO's 2 kbps uplink and 500 kbps downlink rates, a rough estimate of weekly data transfer capability from MRO through the DSN yields 675 MB downlink or 2.7 MB uplink. TGO has similar orbit parameters to MRO, has a DSN downlink rate 150 kbps, and is not capable of uplink. TGO's weekly DSN downlink capability (following the same conventions as MRO's analysis) is 540 MB. Together, the budgeted communication resources on MRO and TGO provide a 1.215 GB downlink (or 2.52 MB uplink, 540 MB downlink) capability through the DSN per week, which exceeds the lander-to-orbiter communications capability. Therefore, the lander-to-orbiter communication capability restricts the amount of data that can be collected per week to 584 MB (leaving margin over the expected 300-400 MB of collected data.)

2) *Data Collection Modes:* There are currently three modes of data collection the lander will operate under, considering the hard weekly data capacity of 584 MB. The first mode will include the operation of all seven instruments on the same day. The second will have reduced science analysis, and the third mode will focus on the solid SAM analysis and geographical analysis. The individual modes are described below:

- 1) The lander will run a single SAM atmospheric analysis, will continuously take EMS data, and will perform five TECP measurements. Additionally, three ChemCam targets will be analyzed, and one image will be taken by both the MastCam and Microscopic Imager for analysis. Lastly, the MLDEX will be run. This mode is planned to run three times throughout an Earth week.
- 2) The lander will run one SAM atmospheric analysis, and the Environment Monitoring System will take measure-

ments throughout the sol. TECP will take 5 measurements and the ChemCam will analyze three targets. This mode is planned to be executed two times per week.

- 3) The SAM unit will take one solid sample analysis, while the EMS takes measurements throughout the sol. TECP will take five measurements, and ChemCam will analyze three targets. The MastCam and Microscopic Imager will take one image each as well. This mode is expected to run two times per seven sols.

The total power consumption for the all of the modes used over the seven-sol cycle is expected to be 7855 W-hr. The total data used during the week is expected to reach approximately 240 Mbytes.

In order to better understand the Martian dust storms the lander will conduct two MLDEX measurements during any dust storms experienced. No other science data will be collected during the storms to conserve power. The total power used by these two measurements is 0.8 W-hr. The data volume consumed will be 75 kilobytes. After these measurements are conducted, the lander will enter a low power mode where only the mission clock will be running until the dust storm subsides. This is not expected to be a significant usage of power or data, thus not jeopardizing the survivability of the lander over the course of the storm.

3) *Hardware:* The avionics package supporting the command and data handling functions will utilize two redundant BAE RAD 5545 single board computers (SBCs) for centralized data processing and storage. A single radiation-hardened SBC contains a RAD 5545 CPU for command processing and payload data along with 1GB of triple modular redundancy (TMR) flash memory, 4 GB SDRAM (synchronous dynamic random access memory), and redundant FPGAs for memory management [59]. The backplane of the SBC is designed to comply with the SpaceVPX standard, which means that RapidIO is used for internal data transfer and SpaceWire is used for control [59]. A single backplane will be shared between the two redundant SBCs. Since most instruments proposed for this mission have flight heritage running on a MIL-STD 1553 data bus, universal reconfigurable translator modules (URTMs) will be required to convert between data bus protocols.

The SBC's standard 4GB SDRAM and 1 GB TMR flash appear to be sufficient for storing the data collected by the science payload between communications downlinks. All mission critical information and instructions will be stored in the non-volatile flash memory, since this information critical to operation is necessary for the mission to proceed following a power loss. Science data will primarily be stored on the volatile SDRAM because it is less crucial to the ongoing success of the mission following a power loss. With a weekly data volume cap of 584 MB, there should be sufficient SDRAM to collect over 6 weeks of data without uplink before it becomes necessary to begin deleting data to make room for more. If risk of power failure over this period without communication is significant (i.e. during a large dust storm), it may be necessary to store science data on the available flash

memory (which will most likely last less than 2 weeks without uplink under a normal data collection schedule.)

Two redundant vectron VT-803 temperature compensated crystal oscillators (TCXOs) have been selected for timekeeping and communication. These oscillators were selected over their oven-controlled counterparts since they are less complex, less energy-intensive, and reliable enough to meet the communications and localization requirements for this mission. The VT-803 exhibits a reliability on the order of 100 ppb over the temperature ranges expected within the warm electronics box, and vectron's oscillators have heritage on previous Mars missions including the Curiosity rover [69].

Figure 23 below outlines a general schematic for the AMERICA cruise stage and lander, highlighting key components and relevant interactions that the C&DH subsystem is responsible for handling. The C&DH hardware will exist within the lander, with necessary connections to the cruise stage where needed. When the cruise stage is jettisoned upon entry into Mars' atmosphere, the C&DH system will remain with the lander as the connections with the removed components are broken.

F. Power

1) Components and Specifications: To provide power for all mission operations, a mission power system composed of solar arrays, batteries, power management and distribution (PMAD), and wiring will be implemented. Solar panels will be used to power the mission in both the cruise stage and upon landing. Solar array details are in table XXIII.

TABLE XXIII
SOLAR ARRAY ATTRIBUTES [40]

Property	Value
Mass/Area (cruise)	7.32 $\frac{kg}{m^2}$
Mass/Area (lander)	2.51 $\frac{kg}{m^2}$
Power Density	437 $\frac{W}{m^2}$
Technology	XTE-SF 3J GaInP/GaAs/Ge
BOL Efficiency	32.2%
EOL Efficiency	30.0%

The cruise stage array is sized to be mounted in the position of operation, eliminating the need for deployment motors. The cruise stage solar array will be jettisoned from the spacecraft in the cruise stage separation of EDL. The solar cells for this stage will be mounted on vented aluminum honeycomb substrate panels.

The landing stage solar array will be deployed as depicted in figure 24 following a successful landing. The solar cells for this stage will be mounted on interconnected triangular substrate panels made from open-mesh Vectran.

A unified power system will be implemented that uses one set of batteries across the spacecraft. Depending on the mission stage, the batteries will be charged by either the cruise stage solar arrays or the lander arrays. The battery system will consist of two eight-cell batteries. The specifications for each individual cell can be found in table XXIV.

TABLE XXIV
BATTERY CELL ATTRIBUTES [42]

Property	Value
Capacity	30 Ah
Specific Energy	141 $\frac{Wh}{kg}$
Operating Temp.	-20 to 60°C

The PMAD will control power through fully regulated Direct Energy Transfer (DET). A regulated system will be used due to the large variation in solar array power/voltage between martian day and nighttime.

2) Budget: The mission components have been described in a power budget that is broken down to Tier 3 elements. The power budget for the various stages of the mission can be found on page 25.

During the cruise phase the spacecraft will have three modes of power operation. The Propulsion Phase will occur when in-flight corrections to trajectory are made. The Communication Phase will happen when information uplink/downlink is occurring. The ADCS Phase will occur when readings are taken using navigation instruments and trajectory corrections are calculated.

Upon landing, there will be three modes of surface power operation. The Science Phase will occur when experiments and instrument observations are made. The Communication Phase is split between downlink and uplink. Between the downlink and uplink communication phases, the downlink power budget was chosen because the downlink phase requires more from the power subsystem. The Rest Phase will cause the lander to enter a low power mode while it is unable to produce power (nighttime). Figure 25 depicts a power profile for surface operations of the AMERICA lander.

G. Launch Vehicle

As a Discovery investigation, AMERICA will be launched as the primary payload on a single launch vehicle. Currently, AMERICA is expected to fall well within the requirements of a standard launch service and will need no additional services beyond the standards offered.

As discussed in Section III-A1, the expected C3 value for the AMERICA mission is approximately $20.5 \frac{km^2}{s^2}$. For launch vehicle analysis, an analogous launch mass estimate was performed using the same launch mass as the Phoenix mission of 700 kg. Additionally, as discussed in section III-C, AMERICA is expected to include a heat shield with a 2 m diameter. With consideration placed on C3, mass, and size, AMERICA will be able to utilize the 5-m low performance class launch vehicles offered by NASA. In the 5-m low performance class range, the final mass of the mission could nearly double and the same launch vehicle would still be adequate. Additionally, if the C3 value is changed by launch delays, a 700 kg mission could still be launched on the same vehicle with a C3 of up to approximately $30 \frac{km^2}{s^2}$.

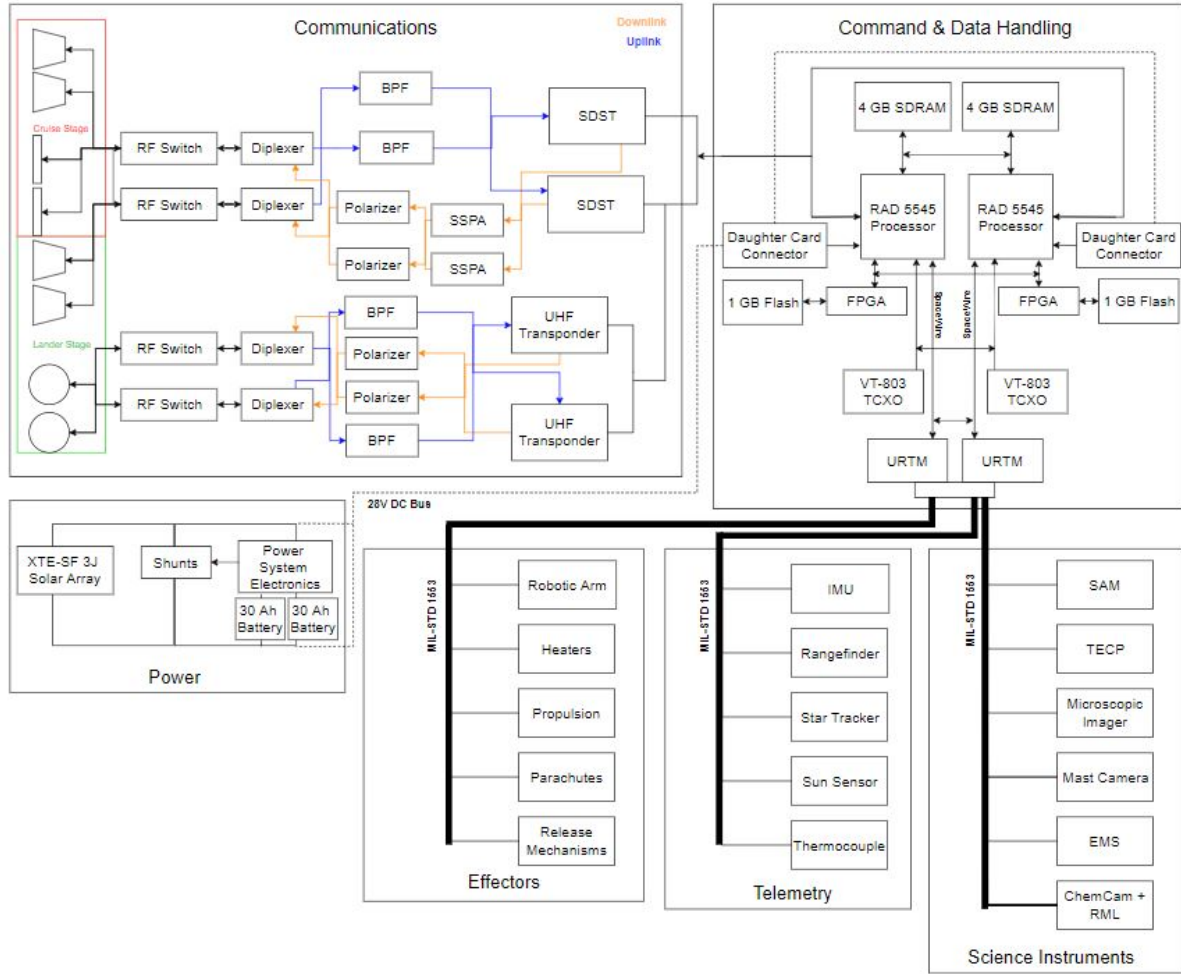


Fig. 23. System interconnect diagram

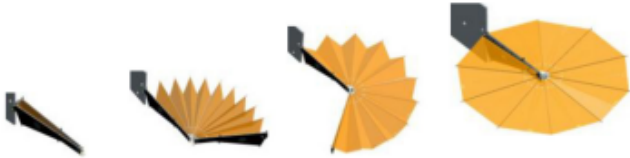


Fig. 24. Deployable Flexible Solar Array sequence that will be used to open solar panels to proper position [41]

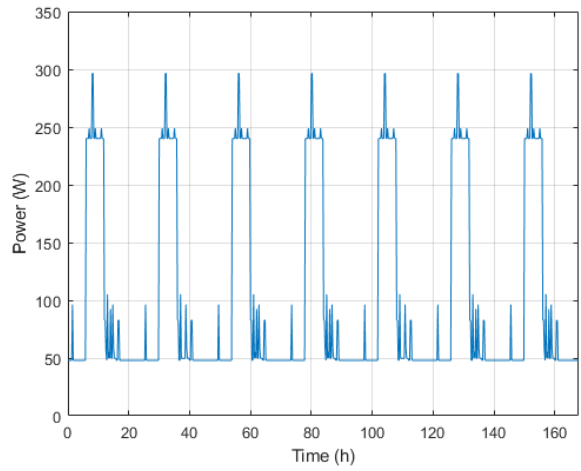


Fig. 25. Power profile of surface operations during cycle of 7 sols

Power Breakdown to Level Three Elements

Element	Peak Power	Standby Power
1.0 Payload		
1.1 Science Instrumentation		
1.1.1 SAM	375	0
1.1.2 Robotic Arm	20	5
1.1.3 EMS	0.015	0
1.1.4 TECP	6.66	0.8
1.1.5 Mastcam-Z (2)	23.6	8
1.1.6 Microscopic Imager	4.3	2.5
1.1.7 Chemistry Camera (LIBS & RMI)	64.7	11.8
1.1.8 Modified Lunar Dust Experiment (MLDEX)	6.11	3.8
2.0 Spacecraft Bus		
2.1 Propulsion		
2.1.1 Cold Gas Thruster (2)	60	0
2.2 ADCS		
2.2.1 CT2020 Star Tracker	28	0
2.2.2 Fine Sun Sensor	28	0
2.2.3 Honeywell MIMS	28	0
2.3 Communications		
2.3.1 X-band Amplifier	65.5	0
2.3.2 Small Deep Space Transponder (X-band)	15.8	0
2.3.3 Electra Lite UHF Transponder	20.6	0
2.4 Power		
2.4.1 PMAD	111.46	0
2.4.2 Wiring	43.47	0
2.6 Thermal Control System		
2.6.1 Electric Heaters	66	0
2.7 C&DH		
2.7.1 Rad 5545 SBC	35	5

*All values have units of watts (W)

Cruise Phase Propulsion Power Budget

Element	Level 2			
	CBE	Contingency	Allocated	Level 1
1.0 Payload (Science Inst.)			0	
2.0 Spacecraft Bus			138.985	
2.1 Propulsion	60	6	66	
2.2 ADCS	0	0	0	
2.3 Communications	0	0	0	
2.4 Power	31.35	3.135	34.485	
2.6 Thermal Control System	0	0	0	
2.7 C&DH	35	3.5	38.5	
3.0 Spacecraft Allocated Power			138.985	
4.0 Margin			41.6955	
5.0 Total Power Available			180.6805	

Cruise Phase Communication Power Budget

Element	Level 2			
	CBE	Contingency	Allocated	Level 1
1.0 Payload (Science Inst.)			0	
2.0 Spacecraft Bus			200.2847	
2.1 Propulsion	0	0	0	
2.2 ADCS	0	0	0	
2.3 Communications	101.9	10.19	112.09	
2.4 Power	45.177	4.5177	49.6947	
2.6 Thermal Control System	0	0	0	
2.7 C&DH	35	3.5	38.5	
3.0 Spacecraft Allocated Power			200.2847	
4.0 Margin			60.08541	
5.0 Total Power Available			260.37011	

Cruise Phase ADCS Power Budget

Element	Level 2			
	CBE	Contingency	Allocated	Level 1
1.0 Payload (Science Inst.)			0	
2.0 Spacecraft Bus			174.097	
2.1 Propulsion	0	0	0	
2.2 ADCS	84	8.4	92.4	
2.3 Communications	0	0	0	
2.4 Power	39.27	3.927	43.197	
2.6 Thermal Control System	0	0	0	
2.7 C&DH	35	3.5	38.5	
3.0 Spacecraft Allocated Power			174.097	
4.0 Margin			52.2291	
5.0 Total Power Available			226.3261	

Surface Science Operations Power Budget

Element	Level 2			
	CBE	Contingency	Allocated	Level 1
1.0 Payload (Science Inst.)			375	
2.0 Spacecraft Bus			174.955	
2.3 Communications	0	0	0	
2.4 Power	124.05	12.405	136.455	
2.6 Thermal Control System	0	0	0	
2.7 C&DH	35	3.5	38.5	
3.0 Spacecraft Allocated Power			549.955	
4.0 Margin			164.9865	
5.0 Total Power Available			714.9415	

Surface Communication Power Budget

Element	Level 2			
	CBE	Contingency	Allocated	Level 1
1.0 Payload (Science Inst.)			31.9	
2.0 Spacecraft Bus			210.8117	
2.3 Communications	101.9	10.19	112.09	
2.4 Power	54.747	5.4747	60.2217	
2.6 Thermal Control System	0	0	0	
2.7 C&DH	35	3.5	38.5	
3.0 Spacecraft Allocated Power			242.7117	
4.0 Margin			72.81351	
5.0 Total Power Available			315.52521	

Surface Rest Power Budget

Element	Level 2			
	CBE	Contingency	Allocated	Level 1
1.0 Payload (Science Inst.)			31.9	
2.0 Spacecraft Bus			17.842	
2.3 Communications	0	0	0	
2.4 Power	11.22	1.122	12.342	
2.6 Thermal Control System	0	0	0	
2.7 C&DH	5	0.5	5.5	
3.0 Spacecraft Allocated Power			49.742	
4.0 Margin			14.9226	
5.0 Total Power Available			64.6646	

IV. MANAGEMENT

A. Risk Classification

The AMERICA mission is classified as Category II based on the categorization guidelines in section 2.1.4 of NPR 7120.5E [61], and the payload falls under risk classification level B based on the guidelines in appendix C of NPR 8075.4 [62].

B. Risk Mitigation

The AMERICA team will use risk mitigation approaches to reduce the probability of risk occurrence, or to adjust the time of risk occurrence in order to ensure successful achievement of all the mission objectives. The process of mitigating risk involves two crucial steps: (1) Identify the steps required in order to reduce the probability and/or effect of an adverse risk, and (2) make a contingency plan to handle risks if they occur.

C. Technical Risk Analysis

Technical risk considers anything which limits the mission's ability to collect data to support the mission objectives. The technical risks the AMERICA lander faces are as follows:

- 1) **The lander does not observe sporadic release of methane within the atmosphere**, resulting in a major loss of data collection to support the science objections. The risk is addressed through the careful selection of the landing site, Medusa Fossae, which has been known to have an abundance of methane in the atmosphere. The addition of geographical methane analysis will provide sufficient science as well.
- 2) **The lander battery is depleted during a dust storm**, and is unable to provide power to survival system. Ultimately this will result in the lander freezing and a mission failure. The risk is mediated with a reduced power usage state during storms in which the lander only supplies the power necessary for its own survival.
- 3) **Landing occurs on hard/rocky/uneven surface and is tilted**. Landing offset would prevent the proper usage of the robotic arm, would reduce the solar panel's exposure to sunlight, and would introduce a tilt that could cause the lander to tip. The introduction of a sky crane during the EDL portion of the spacecraft's flight will help mediate this risk as there will be a landing warning system and a soft touchdown.
- 4) **During landing, the propulsion disrupts the landing area**, causing contamination to the lander surroundings and affecting the reliability of scientific results. The introduction of a sky crane will minimize the amount of disruption to the landing area, thus addressing this risk.
- 5) **The solar panels become covered in dust from the surroundings**, thus lowering the efficiency of the equipment. In turn, this would reduce the amount of power produced for usage and standby. Increased solar panel size and a dust mitigation plan are used to control this risk.
- 6) **The robotic arm fails** due to singularities, loss of power, or significant damage and cannot perform science

collection. By reducing the degrees of freedom the chances of singularity are reduced thus lessening the risk associated with the arm. The risk will also be watched and monitored.

Each risk is plotted within the risk matrix outlined in figure 27 which outlines a risk matrix. The matrix plots the risks based on the probability of occurrence and the severity of the consequences associated with the risk.

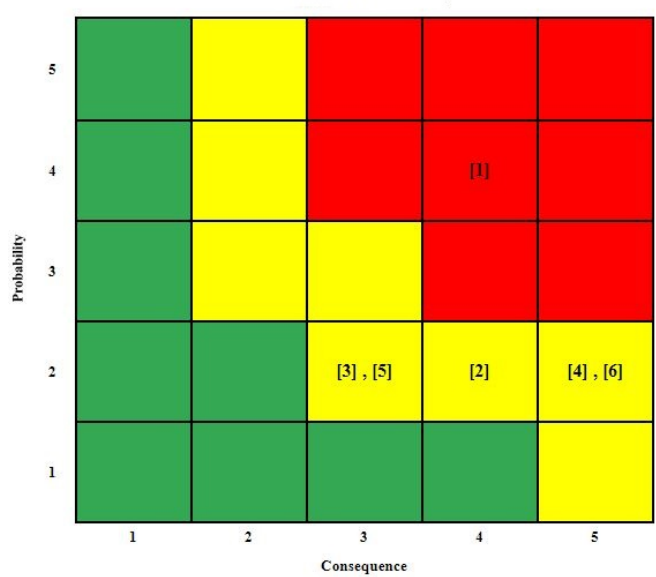


Fig. 27. AMERICA lander risk matrix outlining the priority of the risks based on the severity of consequence and the probability of occurrence

D. Organizational Chart

The AMERICA team is structured following the organizational chart shown in figure 28. The PI (Principal Investigator) is responsible for delegating tasks among the other members, keeping track of the deliverables, and ensuring that the final product is completed within the allotted time. Below the PI are the main divisions that support the mission and include the System Engineer, the Science Team, the Management Team, and the Safety and Quality Assurance lead. Individual members of each team are in charge of the multiple subdivisions that produce the science and technical data needed to support the mission and establish deadlines for each subdivision. Within the four main divisions are separate subdivisions. Under the System Engineer are the Propulsion Control group, Thermal and Power group, Navigation and Landing group, and Mechanical Design group. Tasks within each division are delegated to members on a primary and secondary basis. The members assigned as the primary are responsible for the main research and calculations required to complete the task, as well as making sure that the task is running on schedule. Primaries are supported by one or two secondary members that will aid in the work. A similar structure is continued in the tasks handled by Computing and Data group under the Science Team and in the Cost and Program Management groups under the Management Team. The primary for each task is listed in the Organizational Chart, while the secondaries are not listed.

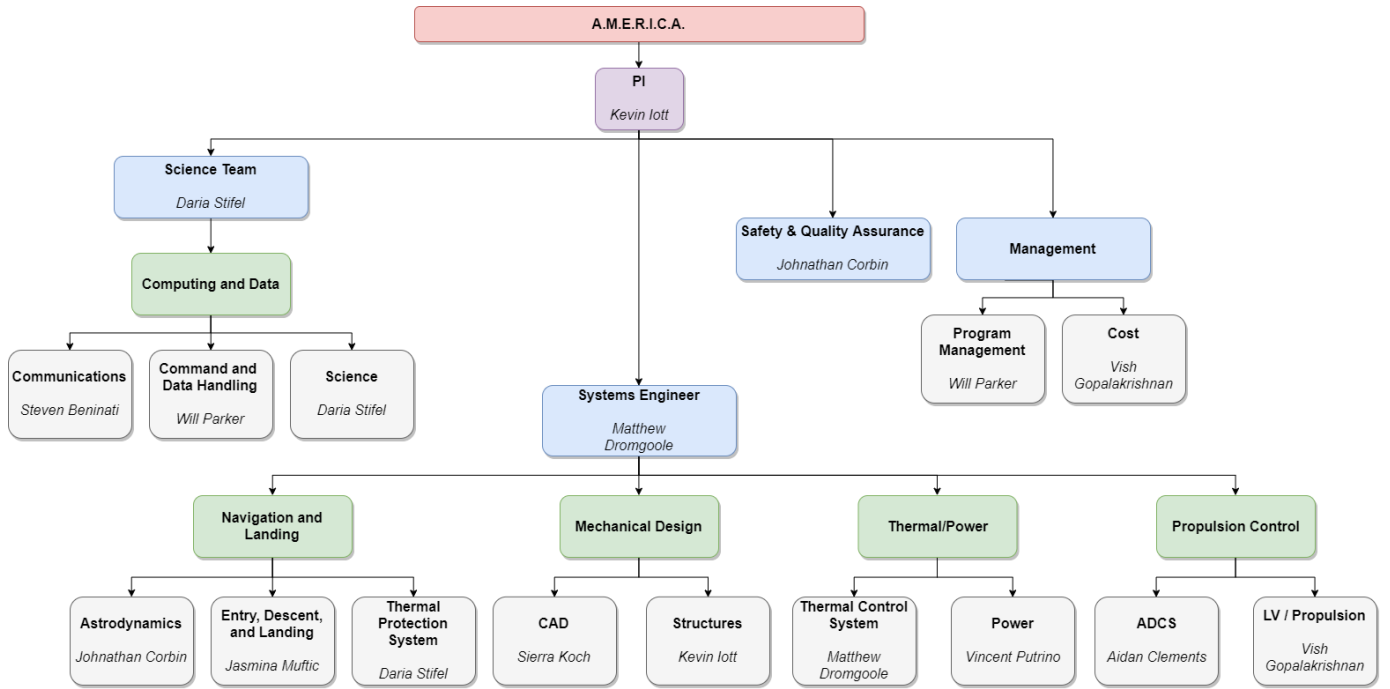


Fig. 28. AMERICA's functional organizational structure promotes communication and teamwork between similar subsystems. To overcome communication barriers between subsystems whole team meetings occurred four times a week.

E. Safety and Quality Assurance

1) *Contamination Control:* In accordance with NPR 8020.12D, AMERICA is classified under a mission planetary protection category of IVb [63]. Under category IV, there exists a significant chance that spacecraft contamination could compromise future investigations interested in the process of chemical evolution and/or the origin of life for the planet the lander resides upon. AMERICA will adhere to the impact avoidance and contamination control set forth in NPR 8020.12D, including cleanroom assembly, microbial reduction, trajectory biasing, and organics archiving.

V. COST AND SCHEDULE

A. Cost Estimate

1) Proposed Mission Cost: The cost of the instruments was estimated using the estimating tools provided in *Space Mission Engineering: The New SMAD*. Each instrument cost takes into account the device's mass, design life (in months), as well as the max power use expected [42]. These variables contributed to each instrument's estimated physical cost, management cost, product assurance cost, and integration and testing cost. The individual costs were then total for each instrument, and summed together is adjusted to inflation. Each subsystem's cost is calculated by summing up components or taking the total mass and using the SSCM (Small Satellite Cost Model) and adjusting the cost to inflation. The communications subsystem, however was modeled with the USCM8 (Unmanned Space Vehicle Cost Model 8) due to the large weight of the sub system. The cost in each subsystem includes both recurring and nonrecurring costs per the SSCM. Along with the cost for the subsystems, wrap factors were calculated with the minimum or average factor determined by priority. The overall cost is \$467,985,315.37 and as the low class launch vehicle is chosen it added \$15M to the maximum budget. \$47,014,684.63 is what is left in reserves in order to accommodate any issues that may happen during production and testing. Table XXV depicts the breakdown of cost per subsystem.

B. Gantt Chart (Full Mission Lifecycle)

The Gantt chart in figure 29 outlines a rough estimate of mission schedule according to the standard NASA mission phase definitions.

TABLE XXV
AMERICA COST MODEL

Sme-SMAD WBS Element	CER in FY19 K Dollars
1.1 Spacecraft	
Science Instrumentation	\$189,571.03
Structures and Thermal Control (Includes Thermal Protection System)	\$39,210.00
Attitude Determination and Control System	\$4,273.00
Electrical Power Supply	\$17,665.82
Propulsion	\$2,683.91
Telemetry, Tracking and Command	\$44,576.00
Command and Data Handling	\$28,058.15
1.2 Spacecraft Integration Assembly and Test	
Integration, Assembly, and Test	\$22,045.46
2.0 Program Level	
Program Level	\$36,319.50
3.0 Flight Support	
Launch and Orbital Operations Support	\$9,674.63
4.0 Aerospace Ground Equipment	
Ground Support Equipment	\$10,467.63
5.0 Wrap Factors	
Annual Operations and Support for Ground Station	\$7,930.02
System engineering	\$-
Project Management	\$-
System Integration and Test	\$-
Product Assurance	\$-
Configuration Management	\$1,586.00
Contractor Fee	\$15,860.04
Data Management	\$1,586.00
Development Support Facility	\$15,860.04
Hardware/ Software Integration	\$4,758.01
Integrated Logistics	\$11,102.03
Safety and Mission Assurance	\$4,758.01
Site Activation	\$4,758.01
6.0 Totals	
Totals in Dollars	\$467,985,315.37
Reserves (\$515 M- Total Cost)	\$47,014,684.63

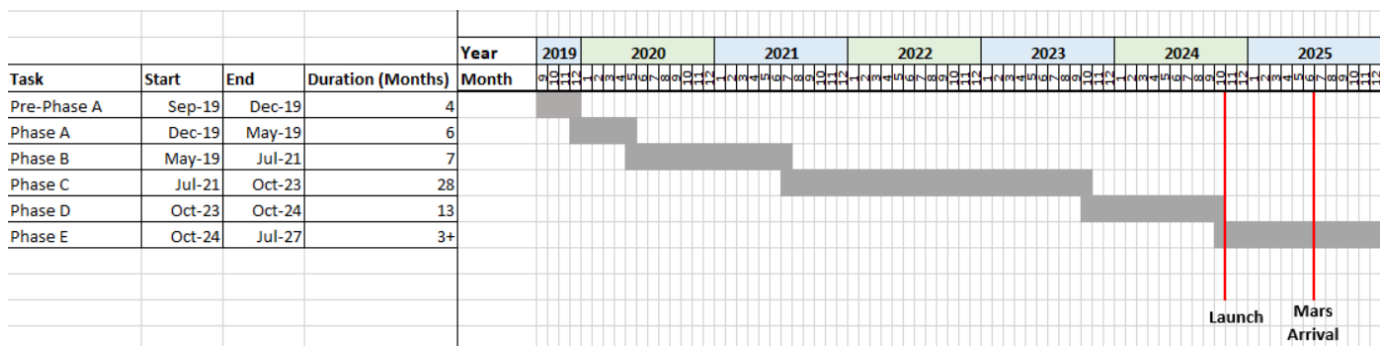


Fig. 29. Gantt chart for full mission schedule of AMERICA

VI. REFERENCES

- 1) Sheppard, J. C., Westberg, H., Hopper, J. F., Ganesan, K., and Zimmerman, P., "Inventory of global methane sources and their production rates," *Journal of Geophysical Research*, vol. 87, 1982, p. 1305.
- 2) Summers, M.E., Lieb, B.J., Chapman, E., and Yung, Y.L. "Atmospheric biomarkers of subsurface life on Mars," *Geophys Res Lett* 29, 2002, doi:10.1029/2002GL015377.
- 3) Giuranna, M., Viscardi, S., Daerden, F., Neary, L., Etiope, G., Oehler, D., Formisano, V., Aronica, A., Wolkenberg, P., Aoki, S., Cardesin-Moinelo, A., Parra, J., Merritt, D., Amoroso, M., "Independent Confirmation of a Methane Spike on Mars and a Source Region East of Gale Crater. *Nature Geoscience*, Vol 12, May 2019, pp. 326–332.
- 4) Oehler, D. Z., and Etiope, G., "Methane Seepage on Mars: Where to Look and Why," *Astrobiology*, Vol. 17, No. 12, 2017, pp. 1233 - 1264.
- 5) Formisano, V., Atreya, S. Encrenaz, T., Ignatiev, N., and Giuranna, M., "Detection of Methane in the Atmosphere of Mars," *Science*, Vol. 306, Issue 5702, 2004, pp. 1758 - 1761. doi: 10.1126/science.1101732
- 6) Webster, C. R., and Mahaffy, P. R., "Determining the Local Abundance of Martian Methane and its 13C/12C and D/H isotopic ratios for Comparison with Related Gas and Soil Analysis on the 2011 Mars Science Laboratory (MSL) Mission," *Planetary and Space Science*, Vol. 59, Issues 2-3, 2011, pp. 271-283. doi: 10.1016/j.pss.2010.08.021
- 7) Gómez-Elvira, J., Armieins, C., Carrasco, I., Genzer, M., Gomez, F., Haberle, R.,, Zorzano, M. (2014), "Curiosity's rover environmental monitoring station: Overview of the first 100 sols," *Journal of Geophysical Research: Planets*, Vol. 119, No. 7, 1680– 1688, doi:10.1002/2013JE004576.
- 8) Wiens, R., and Maurice, S., "MSL Science Corner: Chemistry & Camera (ChemCam)" [retrieved 26 September 2019] <https://msl-scicorner.jpl.nasa.gov/Instruments/ChemCam/>.
- 9) Bell III, J. F., Godber, A., McNair, S., Caplinger, M. A., Maki, J. N., Lemmon, M. T., Van Beek, J., Malin, M. C., Wellington, D., Kinch, K. M., Madsen, M. B., Hardgrove, C., Ravine, M. A., Jensen, E., Harker, D., Anderson, R. B., Herkenhoff, K. E., Morris, R. V., Cisneros, E., and Deen, R. G., "The Mars Science Laboratory Curiosity Rover Mastcam Instruments: Preflight and In-flight Calibration, Validation, and Data Archiving", *Earth and Space Science*, Vol. 4, Issue 7, 2017. doi: 10.1002/2016EA000219
- 10) Arvidson, R., "Phoenix Project Archive Generation, Validation, and Transfer Plan", NASA Jet Propulsion Laboratory, JPL D-29392, February, 2008.
- 11) Herkenhoff, K.; "The Microscopic Imager (MI) of the Spirit and Opportunity Rovers," [retrieved 26 September 2019] <https://mars.nasa.gov/mer/mission/instruments/mi/>
- 12) Sternovsky, Zoltan, "The Lunar Dust EXperiment (LDEX) for LADEE", Laboratory for Atmospheric and Space Physics, Boulder, CO, October 2009.
- 13) Zent, A. P., M. H. Hecht, D. R. Cobos, G. S. Campbell, C. S. Campbell, G. Cardell, M. C. Foote, S. E. Wood, and M. Mehta (2009), "Thermal and Electrical Conductivity Probe (TECP) for Phoenix," *J. Geophys. Res.*, 114, E00A27, doi: 10.1029/2007JE003052.
- 14) Lemmon, M. T., Smith, P., Shinohara, C., Tanner, R., Woida, P., Shaw, A., Hughes, J., Reynolds, R., Woida, R., Penegor, J., Oquest, C., Hviid, S. F., Madsen, M. B., Olsen, M., Leer, K., Drube, L., Morris, R. V., Britt, D., "The Phoenix Surface Stereo Imager (SSI) Investigation", *Lunar and Planetary Science XXXIX*, LPI, No. 1391, March 2008, p.2156
- 15) "NASA's Record-Setting Opportunity Rover Mission on Mars Comes to End," NASA, Release 19-004, Feb. 2019.
- 16) Banfield, D., "MEPAG Mars Science Goals, Objectives, Investigations, and Priorities: 2018", NASA, 2018, <https://mepag.jpl.nasa.gov/reports.cfm>.
- 17) Oze, C., Jones, L. C., Goldsmith, J. I., Rosenbauer, R. J., "Differentiating biotic from abiotic methane genesis in hydrothermally active planetary surfaces," *Proceedings of the National Academy of Sciences of the United States of America*, Vol. 109, No. 25, June 2012, pp 9750-9754.
- 18) Hu R., Bloom, A. A., Gao, P., Miller, C. E., Yung, Y. L., "Hypotheses for Near-Surface Exchange of Methane on Mars," *Astrobiology*, Vol 16, No. 7, 2016, pp. 539-550. DOI: 10.1089/ast.2015.1410
- 19) Ojha, L., Lewis, K., Karunatillake, S., Schmidt, M., "The Medusae Fossae Formation as the single largest source of dust on Mars," *Nature Communications*, No. 2867 (2018), 2018, pp. 1 - 7.
- 20) "NASA Strategic Plan 2018," NASA, 2018.
- 21) Mahaffy, P.R., Webster, C.R., Cabane, M., Conrad, P.G., Coll, P., Atreya, S.K., ..., Mumm, E. "The Sample Analysis at Mars Investigation and Instrument Suite" *Space Science Reviews* (2012) 170: 401. <https://doi.org/10.1007/s11214-012-9879-z>
- 22) Franz, H., "Information Instrumentation for Mass spectrometer", Planetary data system (2013) NASA https://pds-geosciences.wustl.edu/msl/msl-m-sam-2-rdr-l0-v1/mslsam_1xxx/catalog/sam_inst.cat
- 23) "Instrument Overview Phoenix Robotic Arm", Planetary Data System, NASA https://pds-geosciences.wustl.edu/phx/urn-nasa-pds-phx_ra/document/ra_instrument.txt
- 24) Trebi-Ollennu, A., Kim, W., Ali, K., Khan, O., Sorice, C., Bailey, P., ... Lin, J. "InSight Mars Lander Robotics Instrument Deployment System" *Space Science Reviews* (2018) 214: 93. <https://doi.org/10.1007/s11214-018-0520-7>

- 25) Bonitz, R., Shiraishi, L., Robinson, M., Carsten, J., Volpe, R., Trebi-Ollennu, A., Arvidson, R. E., Chu, P. C., Wilson, J. J., Davis K. R. "The Phoenix Mars Lander Robotic Arm," 2009 IEEE Aerospace conference, Big Sky, MT, 2009, pp. 1-12. doi: 10.1109/AERO.2009.4839306
- 26) Shirbacheh, M., Hecht, M., Bell, J. L., Mogensen, C. (2005). "Microscopy, electrochemistry, and conductivity analyzer (MECA) payload on Mars '07 Phoenix lander," 2005 IEEE Aerospace Conference, Big Sky, MT, pp. 279-291. doi: 10.1109/AERO.2005.1559322
- 27) "MECA Instrument Overview", Planetary Data System, NASA https://pds-geosciences.wustl.edu/phx/phx-m-meca-4-nirdr-v1/phxmech_1xxx/catalog/meca_teep_inst.cat
- 28) Herkenhoff, K. E., Squyres S. W., Bell III J. F., Maki, J. N., Arneson H. M., Bertelsen, P., ..., Wadsworth, M. V. (2003), "Athena Microscopic Imager investigation", *J. Geophys. Res.*, 108, 8065, doi:10.1029/2003JE002076, E12.
- 29) J. F. Bell III., J. N. Maki., G.L. Mehall., M.A. Ravine., M.A. Caplinger. "MASTCAM-Z: A Geologic, Stereoscopic, and Multispectral Investigation on the NASA MARS-2020 Rover," Malin Space Systems, Inc., San Diego, CA.
- 30) Harri, A.-M., Genzer, M., Kemppinen, O., Kahanpää, H., Gomez-Elvira J., Rodriguez-Manfredi A., Haberle, R., ... Rennó, N., the REMS/MSL Science Team (2014), "Pressure observations by the Curiosity rover: Initial results", *J. Geophys. Res. Planets*, 119, 82– 92, doi:10.1002/2013JE004423.
- 31) Mihály . Horányi., Zoltán Sternovsky., Eberhard Grün., Ralf Srama., Mark Lankton., David Gathright. (2009) "The Lunar Dust Experiment (LDEX) For the Lunar Atmosphere and Dust Environment Explorer (LADEE) Mission," Laboratory for Atmospheric and Space Physics, University of Colorado, Boulder, CO 80309-0392, USA; <https://www.lpi.usra.edu/meetings/lpsc2009/pdf/1741.pdf>
- 32) Wiens, R.C., Maurice, S., Barraclough, B., Saccoccia, M., Barkley, W. C., ..., Wong-Swanson, B. "The ChemCam Instrument Suite on the Mars Science Laboratory (MSL) Rover: Body Unit and Combined System Tests" *Space Science Reviews* (2012) 170: 167. <https://doi.org/10.1007/s11214-012-9902-4>
- 33) "Cold Gas Thrusters," MOOG Space and Defense, 2018
- 34) "Part Number 80461-1," Northrop Grumman.
- 35) "In-Space Propulsion Data Sheets," Aerojet Rocketdyne, 2019, September
- 36) "Part Number 80148-1," Northrop Grumman.
- 37) "Part Number 80326-1," Northrop Grumman.
- 38) Charles D. Brown "Attitude Control," Elements of Spacecraft Design, edited by John S. Przemieniecki, AIAA, Virginia, 2002, pp. 302
- 39) "LITIS Internal Measurement Unit," UTC Aerospace Systems, 2017
- 40) "XTE-SF Space Qualified Triple Junction Solar Cell" Spectrolab Inc., 12500 Gladstone Avenue, Sylmar California, 91342. https://www.spectrolab.com/photovoltaics/XTE_32_Percent.pdf
- 41) "Ultra-Flex Solar Array Systems" Northrop Grumman Space Components Deployables, 600 Pine Avenue, Goleta, California, 93117. https://www.northropgrumman.com/Capabilities/SolarArrays/Documents/UltraFlex_Factsheet.pdf
- 42) "High Energy long-cycle life and low maintenance lithium-ion cell for demanding applications" EaglePicher technologies, 8225 E. 26th Street, Joplin, MO 64802. <https://www.eaglepicher.com/sites/default/files/LP%2033081%2030Ah%20Space%20Cell%2020040319.pdf>
- 43) M. M. Finckenor. (1999) "Multilayer Insulation Material Guidelines," Marshall Space Flight Center, Marshall Space Flight Center, Alabama, <https://ntrs.nasa.gov/archive/nasa/casi.ntrs.nasa.gov/19990047691.pdf>
- 44) Rinehart, G. H., "Design characteristics and fabrication of radioisotope heat sources for space missions," *Progress in Nuclear Energy*, 2001, pp. 305–319.
- 45) "Mars Exploration Rovers: Rover Temperature Controls" NASA Rept. <https://mars.nasa.gov/mer/mission/rover/temperature/index.cfm#heat-rejection-system>
- 46) Diane K. Fisher., Nancy J, Leon. (2008) "Technologies: Thermal Loop," Accessed 13 October 2019, https://www.jpl.nasa.gov/nmp/st8/tech/heat_pipe_tech2.html
- 47) Cruz, J., and Lingard, J., "Aerodynamic Decelerators for Planetary Exploration: Past, Present, and Future," AIAA Guidance, Navigation, and Control Conference and Exhibit, 2006.
- 48) Edquist, K.T., Desai, P.N., Schoenenberger, M.M. (2008). "Aerodynamics for the Mars Phoenix Entry Capsule." NASA Technical Reports Server.
- 49) "Small Deep-Space Transponder (SDST)," General Dynamics, 2015.
- 50) Pham, T., "Deep Space Network Services Catalog," DSN No. 820-100, Rev. F, February 2015
- 51) Imbriale, W. A., "Technology Drivers," Spaceborne Antennas for Planetary Exploration, Jet Propulsion Laboratory, January 2006, pp. 3-6.
- 52) "X-Band Solid State Power Amplifier (SSPA)," General Dynamics, 2016.
- 53) Brown, C. D., "Telecommunication," Elements of Spacecraft Design, 1st ed, AIAA, inc., Virginia, 2002, pp. 447-499.
- 54) Ulaby, F. T., Ravaioli, U., "Radiation and Antennas," Fundamentals of Applied Electromagnetics, 7th Edition, Pearson Education, inc., New Jersey, 2015, pp. 403-456.
- 55) Griffin, M. D., French, J. R., "Telecommunications," Space Vehicle Design, 2nd ed, AIAA, inc., Virginia, 2004, pp. 511

- 566.
- 56) "Electra-Lite Mars Proximity-Link Communications and Navigation Payload Description," Jet Propulsion Laboratory, April 2019
 - 57) Ho, C., Golshan, N., Kliore, "Radio Wave Propagation Handbook for Communication on and Around Mars," Jet Propulsion Laboratory, JPL Publication 02-5, March 2002.
 - 58) "Mars Relay Description for Discovery 2019 Proposals," Jet Propulsion Laboratory, April 2019
 - 59) "RAD5545 SpaceVPX Single Board Computer," BAE Systems, 2017.
 - 60) Natha, A., Espinoza, L., Greicius, T., "InSight Launch Press Kit," Jet Propulsion Laboratory, Accessed 10
 - 61) "NASA Life Cycles for Space Flight Programs and Projects," NASA Space Flight Program and Project Management Requirements (Updated w/Change 16), NASA, NPR 7120.5E, August 2012.
 - 62) "Appendix B - Classification Considerations for NASA Class A-D Payloads," Risk Classification for NASA Payloads (Updated w/change 3)
 - 63) NASA Procedural Requirements, NPR 8020.12D, April 20, 2011 <https://nodis3.gsfc.nasa.gov/displayDir.cfm?t=NPR&c=8020&s=12D>
 - 64) Kwok, A, "201, Rev. B: Frequency and Channel Assignments", Jet Propulsion Laboratory, 810-005, Rev. E, December 2009.
 - 65) Portock, B. M., Kruizinga, G., Bonfiglio, E., Raofi, B., Ryne, M., "Navigation Challenges of the Mars Phoenix Lander Mission," Jet Propulsion Laboratory, September 2007.
 - 66) Wiliams, W.D., Collins, M., Hodges, R., Orr, R. S., Sands, O. S., Schuchman, L., Vyas, H., "High-Capacity Communications from Martian Distances," NASA, NASA/TM-2007-214415, Springfield, VA, December 2007.
 - 67) "Coarse Sun Sensor," Bradford, 2019
 - 68) "CT2020," Ball Aerospace, 2019
 - 69) "VT-803 Temperature Compensated Crystal Oscillator," Vectron, 2019
 - 70) "Curiosity (Clean)." NASA, NASA, nasa3d.arc.nasa.gov/detail/curiosity-clean.
 - 71) "Entry, Descent, and Landing." NASA, NASA, 8 Aug. 2019, <mars.nasa.gov/msl/timeline/edl/>.
 - 72) "Insight Cruise Lander." NASA, NASA, 7 Nov. 2018, nasa3d.arc.nasa.gov/detail/insight_cruise_lander.
 - 73) Macneill, John. MSL Spacecraft and Skycrane. 10 Sept. 2013, <img2.cgtrader.com/items/28071/55a0fd3446/mars-curiosity-msl-spacecraft-and-skycrane-3d-model-obj-3ds-lwo-lw-lws.jpg>.

VII. APPENDIX

TABLE XXVI
INDIVIDUAL MEMBER CONTRIBUTIONS

Member	Sections Contributed
Steven Beninati	Fact Sheet, II-C, II-D, III-D, III-E
Aidan Clements	Fact Sheet, II-F, III-A5
Johnathan Corbin	Fact Sheet, II-F, III-A1, III-G, IV-D, IV-E
Matthew Dromgoole	Fact Sheet, II-C, III-B, III-F
Vish Gopalakrishnan	Fact Sheet, II-C, III-A4
Kevin Iott	Fact Sheet, II-C, II-E, III-C
Sierra Koch	Fact Sheet, II-A3, II-E5, III-C
Jasmina Muftic	Fact Sheet, II-C, III-A2, IV-B
Will Parker	Fact Sheet, II-A1, II-A2, II-A3, II-C, III-E, IV-A, V-B
Vincent Putrino	Fact Sheet, II-C, II-F, III-A, III-C, III-G
Daria Stifel	Fact Sheet, II-C, II-D, II-E, III-A3, III-E2, IV-C